

Journal of Visualized Experiments

Application of laser micro-irradiation for examination of single and double strand break repair in mammalian cells --Manuscript Draft--

Manuscript Number:	JoVE56265R1
Full Title:	Application of laser micro-irradiation for examination of single and double strand break repair in mammalian cells
Article Type:	Methods Article - JoVE Produced Video
Keywords:	DNA repair; laser micro-irradiation; DNA damage; strand break; XRCC1; gamma-H2AX; strand break signaling
Manuscript Classifications:	4.8.811.74: DNA Repair Enzymes; 5.1.370.350.515.395: Microscopy, Confocal; 5.1.370.350.515.458: Microscopy, Fluorescence; 7.2.111.87.219: DNA Repair; 7.5.355.180: DNA Damage; 7.5.355.195: DNA Repair
Corresponding Author:	Natalie R Gassman, Ph.D. University of South Alabama Mitchell Cancer Institute Mobile, Alabama UNITED STATES
Corresponding Author Secondary Information:	
Corresponding Author E-Mail:	nrgassman@health.southalabama.edu
Corresponding Author's Institution:	University of South Alabama Mitchell Cancer Institute
Corresponding Author's Secondary Institution:	
First Author:	Nathaniel W Holton
First Author Secondary Information:	
Other Authors:	Nathaniel W Holton
	Joel F Andrews
Order of Authors Secondary Information:	
Abstract:	Highly coordinated DNA repair pathways exist to detect, excise and replace damaged DNA bases, and coordinate repair of DNA strand breaks. While molecular biology techniques have clarified structure, enzymatic functions, and kinetics of repair proteins, there is still a need to understand how repair is coordinated within the nucleus. Laser micro-irradiation offers a powerful tool for inducing DNA damage and monitoring the recruitment of repair proteins. Induction of DNA damage by laser micro-irradiation can occur with a range of wavelengths, and users can reliably induce single strand breaks, base lesions and double strand breaks with a range of doses. Here, laser micro-irradiation is used to examine repair of single and double strand breaks induced by two common confocal laser wavelengths, 355 nm and 405 nm. Further, proper characterization of the applied laser dose for inducing specific damage mixtures is described, so users can reproducibly perform laser micro-irradiation data acquisition and analysis.
Author Comments:	
Additional Information:	
Question	Response
If this article needs to be "in-press" by a certain date, please indicate the date below and explain in your cover letter.	

TITLE:

Application of laser micro-irradiation for examination of single and double strand break repair in mammalian cells

AUTHORS & AFFILIATIONS:

Nathaniel W Holton¹, Joel F Andrews¹, and Natalie R Gassman^{1,*}

¹Department of Oncologic Sciences, University of South Alabama Mitchell Cancer Institute, Mobile, AL USA 36604

*Corresponding author: Natalie R. Gassman

Email Address: nergassman@health.southalabama.edu

Tel: (251) 445-8430

Email address of Co-authors:

Nathaniel W Holton (nwholton@health.southalabama.edu)

Joel F Andrews (jandrews@health.southalabama.edu)

KEYWORDS:

DNA repair, laser micro-irradiation, DNA damage, strand break, XRCC1, gamma-H2AX, strand break signaling

SHORT ABSTRACT:

Confocal fluorescence microscopy and laser micro-irradiation offer tools for inducing DNA damage and monitoring the response of DNA repair proteins in selected sub-nuclear areas. This technique has significantly advanced our knowledge of damage detection, signaling, and recruitment. This manuscript demonstrates these technologies to examine single and double strand break repair.

LONG ABSTRACT:

Highly coordinated DNA repair pathways exist to detect, excise and replace damaged DNA bases, and coordinate repair of DNA strand breaks. While molecular biology techniques have clarified structure, enzymatic functions, and kinetics of repair proteins, there is still a need to understand how repair is coordinated within the nucleus. Laser micro-irradiation offers a powerful tool for inducing DNA damage and monitoring the recruitment of repair proteins. Induction of DNA damage by laser micro-irradiation can occur with a range of wavelengths, and users can reliably induce single strand breaks, base lesions and double strand breaks with a range of doses. Here, laser micro-irradiation is used to examine repair of single and double strand breaks induced by two common confocal laser wavelengths, 355 nm and 405 nm. Further, proper characterization of the applied laser dose for inducing specific damage mixtures is described, so users can reproducibly perform laser micro-irradiation data acquisition and analysis.

INTRODUCTION:

Fluorescent microscopy has emerged as a powerful technique to visualize cellular architecture, examine protein localization, and monitor protein-protein and protein-DNA interactions. Using fluorescent microscopy to study DNA damage responses after the application of global DNA damaging agents, such as ultraviolet (UV) light, ionizing radiation, chemical oxidizing or alkylating agents, and/or chemotherapeutics has provided new insight into the initiation, signaling, and recruitment of DNA repair proteins to sites of DNA damage^{1,2}. However, these global and asynchronous damaging events are limiting, if detailed information about the recruitment order, kinetics of association or dissociation, and the relationships between key DNA repair proteins are sought. Fortunately, advancements in laser scanning confocal microscopes, broader availability of damage-inducing laser wavelengths, and improvements in fluorescent proteins over the past 25 years have provided researchers with improved tools for examining these aspects of DNA repair, through targeted DNA damage induction.

Irradiation of cells with laser microbeams in order to study cellular and subcellular functions is a well-established tool in cell and radiation biology³. Application of this technique to the study of DNA repair emerged when Cremer and co-workers used a highly-focused UV (257 nm) laser microbeam system to induce DNA damage over a 0.5 μm spot in Chinese hamster ovary (CHO) cells⁴ and established the induction of DNA photolesions by this system⁵. While offering significant improvements over UV microbeam methods at the time, adoption of this damaging system was limited due to its specialized set up, and its inability to generate double strand breaks (DSBs)⁶. Subsequent investigation of a variety of UV-B (290 – 320 nm) and UV-A (320 – 400 nm) wavelengths by a number of groups revealed that UV photoproducts, oxidative base lesions, single strand breaks (SSBs), and DSBs could be induced dependent on the laser wavelength and power applied^{4,7-10} (reviewed in ³). Further, combinations of these UV-B and UV-A wavelengths with sensitizing agents, like psoralen, bromodeoxyuridine (BrdU), and Hoechst dyes, were also found to induce DNA damage dependent on wavelength, power, and duration of exposure, though the power needed to induce damage is often lowered in the presence of these agents¹¹⁻¹⁵. These advancements expanded the use of micro-irradiation, though there were still technical hurdles to be addressed for wider adoption of these methods.

Cremer and co-workers significantly advanced the field of micro-irradiation by precisely focusing the UV microbeam to apply significant damaging energy over a highly localized area in the cell. As confocal microscopes and laser microdissection systems advanced, tightly focused light was more broadly accessible; however, coupling UV sources to scopes and dealing with the chromatic aberrations they induced still presented significant challenges to most users^{3,6,16}. As UV dyes increased in popularity throughout the 1990s, optics capable of focusing and capturing UV-excited fluorescence became more widely available¹⁶, and improvements in laser scanning offered users the ability to create highly focused UV excitation spots within cells^{6,17}. However, it was not until the early 2000s that the true impact of this combination of tightly focused beams with higher intensity lasers was felt, when numerous reports emerged demonstrating that DNA strand breaks could be induced with and without sensitizers in the UV-A range^{6,10,18-20}, 405 nm²¹⁻²⁶, and even at longer visible wavelengths like 488 nm²⁷. These

advancements allowed for more widespread adoption of the micro-irradiation technique on a number of commercial systems. In parallel with these developments, two-photon techniques also emerged that allowed precise induction of DNA damage; though these advancements will not be discussed here, there are a number of review articles discussing these methodologies^{9,28-}

30.

With the current accessibility of confocal microscopes capable of delivering highly focused UV light and the wide-spread availability of fluorescent proteins to allow real-time tracking of DNA repair proteins, micro-irradiation techniques have evolved into powerful tools for examining DNA damage response and repair pathways. However, users need to be aware that the generation of DNA damage is highly dependent on the laser wavelength and the power applied to the sub-nuclear region. Use of UV-C (~260 nm) wavelengths allow direct DNA excitation and high selectivity for the induction of UV photoproducts^{7,8}. UV-B and UV-A wavelengths produce mixtures of DNA damage (base lesion, SSBs, and DSBs), dependent on the applied power and the cellular background utilized⁷. Endogenous photosensitizers and anti-oxidant levels in the targeted cells can influence the DNA damage mixtures produced by these wavelengths. Additionally, the use of exogenous photosensitizers (BrdU, etc.) may assist in lowering the energy needed for the induction of DNA damage. However, these agents can induce DNA damage by themselves, and they may alter the cell cycle and chromatin structure, so their use may produce undesired effects that need to be considered by the user. Therefore, prior to using micro-irradiation to study DNA damage response and repair, careful consideration of the DNA repair pathway of interest, the wavelengths available for use, and the DNA damage mixture created is required.

Here, laser micro-irradiation is performed at two commonly used wavelengths, 355 nm and 405 nm, without sensitizers to demonstrate the mixtures of DNA damage induced by these wavelengths and the influences these damage mixtures have on examining the repair of SSBs and DSBs. Users should be aware that these wavelengths do not create a single species of strand breaks or base lesions. In order to discriminate between DNA repair pathways, users must carefully control the applied power over a specific region of the nucleus and characterize the induced damage using multiple strand break markers and DNA lesion antibodies. If properly applied and characterized, laser micro-irradiation can enrich some species of DNA damage, allowing users to assess repair of base lesions and SSBs or DSBs, with some specificity. Therefore, we have provided a method allowing users to reproducibly perform laser micro-irradiation, characterize the DNA damage mixtures induced by the applied laser dose, and perform data analysis.

PROTOCOL:

1. Cell Culture and generation of stable cells

1.1 Grow CHO-K1 cells in minimal essential medium supplemented with 10% fetal bovine serum. Maintain cells in a humidified incubator with 5% CO₂ at 37 °C.

1.2 Transfect CHO-K1 cells with 1 µg of plasmid DNA containing human XRCC1 with a C-terminal

green fluorescent protein (GFP) tag using a commercial transfection reagent following the manufacturer's instructions.

1.3 Select CHO-K1 cells stably expressing the human XRCC1-GFP fusion using 800 µg/mL geneticin and enrich the XRCC1-GFP expressing population using fluorescence assisted cell sorting (FACS).

1.4 Plate cells to be micro-irradiated in culture vessels with coverglass bottoms, so they reach approximately 75% or greater confluency on the following day. Some spaces between cells are desirable, particularly if using registration to return to the same image field (described in section 3.2).

2. Microscope set-up

2.1 Select a laser scanning confocal microscope equipped with suitable lasers and optics, and control software for micro-irradiation/photostimulation. Presented experiments use a laser scanning confocal microscope that has been modified to include a 355 nm laser, fiber-coupled to a galvanometer photoactivation miniscanner and controlled using the manufacturer's control and analysis software. This system can perform micro-irradiation in a user-designated region of interest (ROI) using the photoactivation miniscanner (355 nm laser) or the standard confocal galvanometer (405 nm laser).

2.2 Select the wavelength to be used for micro-irradiation, ensuring that all optical components in the micro-irradiation lightpath are suitable for the chosen wavelength.

Note: The presented system uses a 40× C-Apochromat (numerical aperture (NA) 1.2) oil immersion objective together with a UV filter cube for 355 nm micro-irradiation, and a 20× C-Apochromat (NA 0.75) dry objective using the standard confocal lightpath for 405 nm micro-irradiation. The 20× objective used in the setup is not compatible with the 355 nm wavelength; therefore we used the 40× for 355 nm only. Using the dry objective for damaging allows immunofluorescence protocols to be applied downstream without cleaning off immersion oil, which is why we utilize this objective when possible.

2.3 Configure the microscope for the micro-irradiation experiment. To maintain consistency between experiments, designate a standardized configuration of the microscope components to be used for each type of micro-irradiation. Save these settings as a preset within the microscope's operating software, if possible.

Note: In the presented system, cells are micro-irradiated and imaged using unidirectional scanning, a scan resolution of 1024x1024 pixels with 1x scan zoom, at a frame rate of 8 frames per second (fps), and with the pinhole set to approximately 4 Airy Units (AU), as determined for the 488 nm laser (69 µm). This open pinhole setting was chosen to maximize the amount of light captured in each image, allowing the use of lower imaging laser powers and reducing photobleaching.

3. Laser micro-irradiation

3.1 Place the prepared culture dish, containing cells of interest, onto the microscope stage and lock securely into place.

3.1.1. If available, place chambered slide in a stage-top incubator and maintain at 37 °C with 5% CO₂ during damage induction. This step is most important for live-cell timelapse imaging or long imaging sessions. Otherwise place cells on the microscope stage and perform irradiation at room temperature (~ 25 °C), and then quickly return cells to an incubator at 37 °C with 5% CO₂.

3.2. Register image fields to allow the researcher to return to the same location after performing fixation, staining, or other procedures. Perform registration of damaged fields using an encoded, automated microscope stage or cell culture coverglass vessels with an etched or labeled grid of XY locations.

3.2.1. If using software image registration, select a recognizable feature of the culture vessel (i.e., the corner of the coverglass or barrier between wells), collect an image, and record the XY location. This will allow for alignment and registration of the XY locations of selected fields following sample preparation.

3.2.2. If using manual registration, record grid or etched locations for each field manually, being careful to record the orientation and placement of the dish on the stage.

3.2.3. If no identifying features for the cell culture vessels are available, identify damaged fields by visual inspection of cell morphology and density. Take care to select fields with sufficiently distinct features to be recognizable during later imaging.

Note: This can be time consuming to perform unless the orientation and area of the culture vessel is tightly restricted.

3.3. Select a field for micro-irradiation and focus the sample. For cells expressing fluorescently labeled proteins, select the focal plane with the maximal nuclear cross-section in the fluorescent channel of interest. For cells not expressing labeled proteins, or for those without clear nuclear localization, phase contrast or differential interference contrast (DIC) imaging can be used to find the correct focal plane.

Note: A useful feature of phase contrast and DIC imaging is the fact that as the focal plane moves through the sample, the same feature can appear light or dark depending on the relative focal plane.

3.3.1. Select a clear feature within the nucleus, such as a nucleolus, and move the focal plane up and down while observing this change in appearance. The true focal plane will lie within the transition from light to dark. To focus the sample, select the focal plane in which the selected feature has the sharpest contrast.

3.4 Register the position of the field of interest. Create a 3x3 pixel square ROI within the microscope software, place this ROI over the nucleus of a cell to be damaged, and set this ROI to be the damage ROI.

3.5. Collect a pre-damage image, including the position of the damage ROI.

3.5.1. For experiments that do not use fluorescent proteins, acquire a phase-contrast or differential interference contrast (DIC) brightfield image to identify and record nuclei for damage.

3.5.2. For live-cell experiments using fluorescent proteins, acquire an image containing brightfield and the fluorescence channel for the protein of interest (i.e., laser line 488 nm for excitation of GFP, laser line 561 nm for excitation of RFP). In experiments using the CHO-K1 XRCC1-GFP, fluorescence excited by the 488 nm laser line was simultaneously collected with the transmitted DIC brightfield channel.

3.6. Initiate laser damage.

3.6.1. In the presented system, control the laser dose by the total time spent scanning the damage ROI. Because the galvanometer for the 355 nm laser operates at a fixed scan rate, laser dose is controlled by the time spent repeatedly scanning the selected damage ROI: in the data presented here, micro-irradiation at 355 nm is performed for 2 and 10 seconds.

3.6.2. In contrast, control the 405 nm laser dose by modulating the scan rate and perform one scan of the selected damage ROI. In the data presented here, use 8 and 0.5 fps for micro-irradiation at 405 nm. A scan rate of 8 fps delivers a lower laser dose than 0.5 fps, because the laser spends less time on each pixel during the scan. Both lasers are operated at 100% power. See section 3.7 for instructions on measuring laser power directly.

Note: Each individual microscope system may differ in how laser power is delivered to a designated ROI, similar to how the 355 nm and 405 nm differ in the presented system. Users will need to determine this procedure for their microscope system and report these parameters within their methods sections.

3.6.1. For live cell imaging, perform timelapse image acquisition of brightfield and fluorescence channels. Adjust duration and frequency of timelapse to optimize data collection, ideally capturing the accumulation of the fluorescent protein at the damage ROI and its dissociation over the time course of the experiment. Experiments using XRCC1-GFP collected images every 30 seconds for 20 minutes.

Note: The frequency of the timelapse imaging can be limited by photobleaching of the fluorophore, complicating analysis of accumulation and dissociation. Photobleaching can be evaluated by observing undamaged cells during the timelapse and adjusting acquisition conditions to minimize fluorescent signal loss in these undamaged cells. Some photobleaching

may be unavoidable, so users may compensate for the signal loss by normalizing the fluorescent intensities of damaged cells to those of undamaged cells in each frame of the timelapse.

3.6.1.1. After the time course is completed, select a new field of cells for damage or fix damaged cells for further analysis, as described in section 4.

3.6.1.2. Continue micro-irradiation and timelapse imaging until the desired number of damaged cells is reached.

Note: We recommend damaging a total of 10-25 cells per selected condition in order to assess the cell-to-cell heterogeneity in response to the induced damage. Although most confocal systems will allow users to damage more than one cell during each micro-irradiation, this introduces staggered damage initiation times, which can complicate analysis of peak recruitment time over a large number of cells or dissociation time for fast events. In some systems, simultaneous damage induction over several ROIs may reduce the laser dose received by each independent ROI. Therefore, unless these timing/power issues are directly addressed by the user, it is recommended that cells be damaged individually.

3.6.2. For analysis by immunofluorescence (IF), perform damage and either immediately fix cells, as described in section 4, or allow cells to repair for selected increments of time (i.e., 1, 5, 10 or 20 min). After the desired time elapses, fix and stain the cells, as detailed in section 4.

3.6.2.1 To increase overall cell number for IF analysis, damage additional fields within the culture vessel to generate a multi-field time course of the post-damage response. Record the XY location of each field and the time that the damage occurred. After the desired total repair time elapses, fix and stain the cells as detailed below.

3.7. After observing of protein recruitment at selected doses, measure and report laser power levels post-fiber and post-objective to accurately characterize and report laser doses. We use a compact digital power meter and two different photodiode sensor heads; one coupled directly to the laser fiber to measure post-fiber output, and the other placed on the microscope stage to measure post-objective output.

3.7.1. To measure laser power, place the sensor in the desired configuration (post-fiber or post-objective) and perform micro-irradiation as described above, while recording the measurements made by the power meter. Be aware that the sampling rate of the power meter may not be fast enough to capture very rapid micro-irradiation events, so it may be necessary to run multiple iterations of the experiment to ensure that the power meter accurately detects the applied dose.

Note: For the 355 nm laser, we measured an average peak power of approximately 5 mW post-fiber and approximately 19 μ W post-objective. For the 405 nm laser, micro-irradiation was performed in loops of 30 iterations to overcome the 0.01 s maximum sampling rate of the

power meter, and average peak powers of 1.5 mW and 2.4 mW were measured using scan speeds of 8 and 0.5 frames per second, respectively. Every power meter is different. Users will need to determine the operational wavelengths and sampling rates for their individual power meter.

4. Immunofluorescence staining procedures

4.1. Analyze strand break induction by IF staining.

4.1.1. Fix cells with 3.7% formaldehyde (CAUTION) in phosphate buffered saline (PBS) for 10 min. Aspirate formaldehyde solution and wash 3 times with PBS. The protocol can be stopped here by placing PBS back on the cells, and the cells can be stored at 4 °C for up to 1 week.

CAUTION: Formaldehyde is toxic and carcinogenic. Wear proper personal protective equipment and dispose of the toxic substance as instructed by institutional environmental health and safety procedures.

4.1.2. Permeabilize cells using 0.25% Triton X-100 in PBS for 10 min at room temperature (RT) and then wash 3 times with PBS.

4.1.3. Block non-specific antibody binding by incubating for 30 min in PBS containing 1% bovine serum albumin (BSA) at RT.

4.1.4. Incubate with primary monoclonal antibody against γ H2AX and primary polyclonal antibody against 53BP-1 both diluted 1:750 in PBS containing 1% BSA for 1 h at RT, and then wash 3 times with PBS.

4.1.5. Incubate cells with Alexa 488 goat anti-mouse and Alexa 546 goat anti-rabbit both diluted 1:2000 in PBS containing 1% BSA for 1 h at RT, and then wash 3 times with PBS.

4.1.6. Stain nuclear DNA with a 10 mg/mL solution of DAPI (4',6-Diamidino-2-Phenylindole, CAUTION) diluted to 1:5000 in PBS for 5 min, or use comparable nuclear dye, and then wash 3 times with PBS.

CAUTION: DAPI is toxic and mutagenic. Wear proper personal protective equipment and dispose the toxic substance as instructed by institutional environmental health and safety procedures.

4.1.7. Place PBS or PBS + 0.1% sodium azide (CAUTION) back onto the stained cells. Protocol can be stopped here and cells stored at 4 °C for several days, or proceed to image acquisition in section 5.

CAUTION: Sodium azide is toxic. Wear proper personal protective equipment and dispose the toxic substances as instructed by institutional environmental health and safety procedures.

4.2. Analyze induction of base lesions or DNA adducts by IF staining.

4.2.1. Fix and permeabilize cells in ice-cold methanol (CAUTION) for 20 min at -20 °C.

CAUTION: Methanol is toxic and flammable. Wear proper personal protective equipment and dispose the toxic substance as instructed by institutional environmental health and safety procedures.

4.2.2. Aspirate the methanol and allow the sample to dry completely for 15 min. Protocol can be stopped here and cells stored at -20 °C dry for up to 3 days.

4.2.3. Rehydrate the cells in PBS for 15 min.

4.2.4. Denature DNA using 2 N HCl (CAUTION) for 45 min at RT and wash 3 times with PBS.

CAUTION: HCl is corrosive. Wear proper personal protective equipment and dispose the corrosive substance as instructed by institutional environmental health and safety procedures.

4.2.5. Neutralize in 50 mM Tris-HCl pH 8.8 for 5 min followed by 3 washes with PBS.

4.2.6. Incubate cells in blocking buffer made with 5% normal goat serum and 0.1% Triton X-100 in PBS for 1 h at RT.

4.2.7. Incubate with primary antibodies for 8-oxo-2'-deoxyguanosine (8-oxodG, 1:400) or cyclobutane pyrimidine dimer (CPD, 1:1000) in the goat serum blocking buffer for 1 h at RT, and then wash 3 times with PBS.

4.2.8. Incubate cells with Alexa 488 goat anti-mouse at a 1:2000 ratio in the goat serum blocking buffer for 1 h at RT, and wash 3 times with PBS.

4.2.9. Stain nuclear DNA using 1:5000 DAPI (10 mg/mL) in PBS for 5 min, and wash 3 times with PBS.

4.2.10. If using chambered coverglass, place PBS or PBS + 0.1% sodium azide back onto the stained cells. Protocol can be stopped here and cells stored at 4 °C for several days, or proceed to image acquisition in section 5.

4.2.11. Alternatively, mount cells in preferred mounting medium, if an additional coverglass can be placed on top of the culture vessel. Once cured, mounted cells can be stored at 4 °C for long periods of time.

5. Image acquisition for immunofluorescence experiments

5.1 Clean the coverglass bottom of the culture vessel with ethanol and place it back on the confocal microscope stage. Ensure that the orientation and position of the vessel on the stage

corresponds to the orientation and position recorded when damage was induced. Secure the culture vessel to ensure optimal registration and imaging.

5.2. Locate previously imaged fields using the registration technique selected (described in 3.2).

5.2.1. For manual registration using a coverglass with an etched grid, bring the grid into focus and find identifying marks. Then use recorded XY coordinates to locate damaged cells.

5.2.2. For image-based automated registration, locate the structural feature used as a reference in step 3.2.1, and then align the current live microscope view as closely to the recorded image as possible. Once aligned, measure the current XY microscope stage location and compare it to the XY location of the reference image. The linear distance between the two locations defines the X and Y offset. Apply this offset to each recorded XY location to identify the image field(s) containing the irradiated cell. This offset function may be automated in the microscope control software or performed manually.

5.2.3. If no appropriate registration points could be identified, manually locate cells by scanning the slide and locating the previously identified cell features.

5.3. Acquire images using appropriate microscope settings to collect all stained targets, including a brightfield image (setting in section 2.3 and focusing in section 3.3). In presented experiments, multichannel images were collected using the following excitation laser lines and fluorophores: 405 nm (DAPI), 488 nm (Alexa 488 and transmitted DIC brightfield), and 561 nm (Alexa 546). All lasers pass through a single acousto-optical tunable filter controlling the transmission of both laser wavelength and power.

6. Live cell image analysis of the recruitment of fluorescent proteins to micro-irradiated sites

6.1. Open acquired images in an image analysis application (i.e., NIS Elements or ImageJ). If necessary, combine the pre-irradiation image with timelapse images to generate a single image sequence of pre- and post- damage induction. Users can show recruitment by measuring changes in fluorescent intensity over the irradiated area relative to the fluorescence intensity measured across the whole nucleus (see Representative Results Figure 1B).

6.2. For each cell to be measured, first generate a reference ROI that represents the nucleus. Use a thresholding algorithm on the fluorescent signal that contains the pixels making up the nucleus, and then convert this area into a ROI. If necessary, the ROI can be manually drawn in using the brightfield as a reference. Adjust the ROI over the time course to ensure the nuclear area is accurately covered by the ROI, and report the mean fluorescence intensity of the fluorescent signal within this ROI for each frame.

6.3 For each cell to be measured create a 6x6 pixel ROI and place it over the damage ROI for each frame of the time course. This larger ROI is now the damage ROI for analysis. Report the mean ROI fluorescence intensity for each frame.

NOTE: Most commercial image analysis software contains modules for 2D object tracking, and there are a number of user-developed macros for ImageJ or FIJI that facilitate faster workflow and higher throughput (see <https://imagej.nih.gov/ij/plugins/>).

6.4. Normalize the mean damage ROI fluorescence intensity to that of a corresponding reference ROI in each frame of the timelapse. Here, the mean nuclear fluorescence intensity is used as the reference ROI (see Representative Results Figure 1). Normalization can be performed by subtracting the mean reference ROI fluorescence intensity from the mean ROI fluorescence intensity, or by dividing the mean damage ROI fluorescence intensity by the mean reference ROI fluorescence intensity.

Note: Normalization by division can yield unpredictable results, if used in situations with very low reference intensity values.

6.5. Repeat for all damaged cells, as well as for at least two control, undamaged cells. Control cell results can be used for further normalization, if required.

6.6. Graph normalized intensity values over time to show changes in recruitment dynamics as a function of experimental treatment.

7. Image analysis of protein recruitment detected by immunofluorescence

7.1. Open pre- and post-damage images in an image analysis application. The pre-damage images contain the damage ROI(s) used for micro-irradiation. Copy the ROI(s) and paste into the post-damage images to identify targeted cells.

7.2. Generate a 6x6 pixel ROI for analysis of protein recruitment and place this ROI at the location of the damage ROI. This larger ROI is now the damage ROI for analysis. Report the mean damage ROI fluorescence intensity.

7.3. Normalize the mean damage ROI fluorescence intensity to that of a corresponding reference ROI. Here, the mean nuclear fluorescence intensity of the damaged cell is used as the reference ROI (see Representative Results Figure 1). Generate the reference ROI by using a thresholding algorithm on the DAPI signal to define the nucleus, and then convert this area to a ROI. Report the mean reference ROI fluorescence intensity. Normalization can be performed by subtracting the mean reference ROI fluorescence intensity from the mean damage ROI fluorescence intensity, or by dividing the mean damage ROI fluorescence intensity by the mean reference ROI fluorescence intensity.

Note: Normalization by division can yield unpredictable results, if used in situations with very low reference intensity values.

7.4. Repeat for all damaged cells, and perform the same analysis on at least two control cells, as described above.

7.5. Graph normalized intensity values for each measured micro-irradiation event against time to show changes in protein recruitment or type of DNA damage as a function of experimental treatment.

REPRESENTATIVE RESULTS:

Characterization of induced DNA damage

Induction of base lesions and strand breaks is dependent on the laser dose applied to the selected nuclear area and the cellular microenvironment of the cell model used⁷. Fluorescent proteins fused to repair proteins, like XRCC1, 53BP1, Ku70, or Rad51, provide useful single and double strand break markers for establishing the minimal energy required to see accumulation of a fluorescent protein within a damage ROI above the background fluorescence^{9,19,31}. Once conditions that induce a response are found, it is critical to characterize the damage mixture induced by that specific wavelength and dose. Attenuation of the dose and duration at the wavelength used can allow the user to minimize the formation of complex damage mixtures. Low laser doses in the UV-A range have been demonstrated to produce predominantly SSBs and a small amount of base lesions, appropriate for studying SSB and BER pathways^{10,28}. Increasing the dose creates more complex base lesions, oxidative and UV induced, and induces more significant numbers of DSBs^{7,10}. While the induction of a single species of DNA damage is desirable for examination of specific DNA repair pathways, it is more likely that users are inducing a mixture of DNA lesions, with a specific lesion like SSBs being much more frequent than base lesions or DSBs. This is similar to DNA damage mixtures induced by chemical agents like hydrogen peroxide (H₂O₂) or methyl methanesulfonate (MMS)³². Users need to be aware when they report results that damage mixtures can occur, and careful characterization of the dose and lesions at the induced damage site are necessary to ensure the reproducibility and comparability of their results.

In micro-irradiation studies, XRCC1-GFP is often used as a marker for the induction of base lesions and SSBs^{9,28}. XRCC1 is a scaffold protein that plays an important role in SSB repair (SSBR) and base excision repair (BER), and also participates in other repair pathways, like nucleotide excision repair (NER)³³⁻³⁵. It plays an important coordinating role in DNA repair, interacting with a number of key proteins, including poly(ADP-ribose) polymerase 1 (PARP-1), DNA polymerase β (Pol β), and DNA ligase III. We utilized XRCC1-GFP stably expressed in CHO-K1 cells to determine the laser doses required to generate SSBs and DSBs. We first identified the minimum dose required to induce an observable recruitment of XRCC1-GFP for each wavelength (Figure 1). For the 355 nm wavelength, a 2 s dwell time over the defined damage ROI generated an increased fluorescent signal within that ROI, indicating the induction of DNA damage that was detectable over the background (Figure 1A). For 405 nm, an 8 fps scan rate was needed to generate an observable recruitment to the damage ROI (Figure 1A). The dose was then increased (10 s for 355 nm and 0.5 fps for 405 nm) to create a more intense damage ROI (Figure 1A).

Recruitment and retention of XRCC1-GFP at the site of induced damage was then monitored by timelapse imaging. Retention of the protein at the site of DNA damage may indicate on-

going DNA repair, while dissociation of the protein from the site of induced damage is often considered a marker for completion of BER or SSBR. However, there has been no clear evidence linking the dissociation of XRCC1 from laser-induced DNA damage sites with the completion of repair. Recruitment of the protein to the site of damage is measured by reporting the mean intensity of the fluorescent signal within the damaged ROI over the mean fluorescent signal measured for the entire nucleus (Figure 1B). This type of normalization helps address intensity fluctuations in the nuclear signal, though other normalization techniques can be employed depending on the cellular distribution of the protein of interest. Here, XRCC1 is localized in the nuclear compartment, so normalization to the nuclear area measures the redistribution of the signal to the damage ROI. The ROI mean fluorescent intensity is then recorded for each image in the timelapse, including the pre-damage image, and graphed as a function of time (Figure 1C).

We then further characterized the damage induced by the two selected laser doses to examine the formation of DNA base lesions. First, formation of CPD, a bulky UV-induced lesion, was probed by immunofluorescence as a marker for NER type lesions (Figure 2A). Then, the oxidatively induced base lesion 8-oxodG was probed as a marker for BER type lesions (Figure 2B). No significant increase in CPD lesions were observed at the low dose exposure for both wavelengths (2 s for 355 nm and 8 fps for 405 nm), while the high dose treatment at both wavelengths (10 s for 355 nm and 0.5 fps for 405 nm) did show a significant increase in fluorescent signal observed within the damage ROI (Figure 2A). A scatter plot of the CPD ROI mean intensity for each damaged cell shows heterogeneity in damage formation and detection at both wavelengths and doses, indicating that a low level of CPD lesions may be present at the lower doses, but the load may not be significantly detected until a higher dose is applied. The scatterplot also suggests that inefficiency in antibody detection that may limit accurate quantification of the damage mixtures.

This is further highlighted in the detection of oxidatively induced DNA lesions by the marker 8-oxodG. No clear increase in fluorescent signal within the damage ROI was observed for 8-oxodG at either laser wavelength or dose used (Figure 2B). The antibody used for this work is consistent with previous publications^{9,10,36}; however, it should be noted that there can be limitations in observing the formation of 8-oxodG with antibodies^{37,38}. Confirmation of the lack of oxidatively induced lesions is also recommended by a second marker, like recruitment of 8-Oxoguanine DNA Glycosylase (OGG1), the enzyme responsible for removal of 8-oxodG from the DNA¹⁰. We did not observe OGG1 recruitment to our DNA damage sites; however, the formation of low levels of oxidatively induced DNA damage cannot be ruled out completely.

Finally, we examined the formation of DSBs using two markers, γ H2AX and 53BP-1, at the selected laser doses by immunofluorescence (Figure 3 & 4). γ H2AX is commonly used as a strand break marker, but its specificity for DSBs has been questioned in a number of reports^{39,40}. Additionally, it is a phosphorylation event that propagates from the strand break site, so localization of the signal to a strand break can be limited due to this signal propagation. Therefore, combining γ H2AX with 53BP-1 allows for more accurate assessment

of DSB formation within the damage ROI.

The response of γ H2AX and 53BP-1 to micro-irradiation is both wavelength and dose dependent. The low dose (2 s) stimulation at 355 nm elicits no response at 5 and 20 min, and a weak and variable response 10 min post irradiation (Figure 3A) for both markers. The high dose (10 s) of 355 nm micro-irradiation induces an increased fluorescent signal within the damage ROI at 5, 10, and 20 min post irradiation that is reduced at 40 min (Figure 3B). These results indicate that careful titration of the 355 nm dose is required to minimize cross-stimulation of repair pathways, as demonstrated by the reduced detection of the double strand break marker γ H2AX at the early time points (< 20 min) at the low dose applied.

Similar experiments were performed using both low (8 fps) and high dose (0.5 fps) 405 nm laser stimulation (Figure 4). At this wavelength significant accumulation of fluorescent intensity within the damage ROI was observed for both 53BP-1 and γ H2AX regardless of applied dose, indicating that these doses generate a complex mixture of single and double strand breaks almost immediate after the induction of DNA damage (Figure 4). Additionally, the high doses of 405 nm show an increase in pan-nuclear γ H2AX staining within 10 min of damage induction (Figure 4B, bottom) that makes detection of the damage ROI difficult to report, while the 53BP-1 accumulation is more contained within the damage ROI.

These results clearly demonstrate that 405 nm micro-irradiation is not appropriate for monitoring SSB or BER, and that multiple markers for DNA adducts and strand breaks should be employed to fully characterize the induced lesions and DNA repair responses.

Dose-dependent alteration in recruitment and retention of XRCC1-GFP

Once the induced DNA damage has been characterized, laser micro-irradiation can be an ideal platform for studying the dynamics of DNA repair proteins. The retention and dissociation kinetics of the XRCC1-GFP shows a dose dependency (Figure 1), which is not unexpected given the induction of different damage mixtures by each wavelength. The highest irradiation doses (10 s and 0.5 fps) show a higher intensity recruitment of XRCC1-GFP relative to the lower doses and longer retention of the XRCC1-GFP at the site of damage over the 20 min time course (Figure 1C). This indicates that the DNA damage created at higher doses for both 355 and 405 nm is likely not resolved during the course of the experiment, which is consistent with the appearance and retention of DSB markers, γ H2AX and 53BP-1 (Figures 3 & 4).

Interestingly, the lower damage doses (2 s and 8 fps) show rapid recruitment of XRCC1-GFP to the damage sites and dissociation of XRCC1-GFP over the experimental time course to pre-irradiation levels (Figure 1C). Without the complete characterization of the damage mixture, this may lead to the conclusion that SSBs and base lesions are completely resolved using these damaging conditions. However, the presence of γ H2AX and 53BP-1 at 40 min for 355 nm and at 5 min for the 405 nm may lead to different interpretations. For the 355 nm 2 s dose, the damage mixture may be predominantly SSBs, so the appearance of DSB markers at 40 min may indicate that some unrepaired lesions may be leading to DSBs or that DSBs

generated by this energy are repaired on a longer time scale. Time scale differences between SSBR and DSB repair have been previously reported^{28,41,42}. Similarly, the 405 nm low dose (8 fps) dissociation may indicate a low level of SSBs or a clustering of SSBs that are rapidly converted to DSBs, which has been noted for high damage micro-irradiation and other DNA damaging agents previously⁴³⁻⁴⁵.

Together these results highlight the importance of characterizing the induced damage mixtures and utilizing multiple DNA repair proteins and markers for interpreting the recruitment and retention of DNA repair proteins at sites of induced damage.

Figure 1. Laser micro-irradiation induces recruitment of XRCC1-GFP.

(A) CHO-K1 cells stably expressing XRCC1-GFP were irradiated and imaged before and immediately after damage induction. Arrows indicate location of micro-irradiation dose and scale bar is 10 μ m. (B) Recruitment is measured by determining the mean fluorescent intensity within the damage ROI and normalizing to the mean fluorescent intensity of the entire nucleus. (C) Dynamics of recruitment can be measured for each timelapse image. Graphs are representative of two independent experiments with error bars representing the SEM (n=24).

Figure 2. Laser micro-irradiation induces nucleotide damage.

CHO-K1 cells were subjected to laser micro-irradiation and fixed immediately after damage induction. Immunofluorescence was performed to detect CPD and 8-oxodG adducts. (A) Top, scatter plot of the ROI mean fluorescence intensities observed in damaged cells after CPD staining. Bottom, representative images of CPD staining. Arrows indicate location of micro-irradiation and the scale bar is 10 μ m (n=12). (B) Representative images for 8-oxodG staining. Arrows indicate location of micro-irradiation and the scale bar is 10 μ m.

Figure 3. DNA double strand break markers respond to 355 nm micro-irradiation in a dose dependent manner.

CHO-K1 cells were subjected to micro-irradiation and fixed at the time points indicated post-stimulation. Immunofluorescence for the DSB markers γ H2AX and 53BP-1 was performed. (A) Scatter plot of normalized damage ROI mean fluorescence intensities measured for undamaged and damaged cells. Error bars are representative of the SEM (n=12). (B) Representative images for γ H2AX and 53BP-1 staining. Arrows indicate location of micro-irradiation and the scale bar is 10 μ m.

Figure 4. DNA double strand break markers robustly respond to 405 nm micro-irradiation.

CHO-K1 cells were subjected to micro-irradiation and fixed at the time points indicated post stimulation. Immunofluorescence for the DSB markers γ H2AX and 53BP-1. (A) Scatter plot of normalized damage ROI mean fluorescence intensities measured for undamaged and damaged cells. Error bars are representative of the SEM (n=12). (B) Representative images for γ H2AX and 53BP-1 staining. Arrows indicate location of micro-irradiation and the scale bar is 10 μ m.

DISCUSSION:

Using the conditions described here, any confocal microscope with a UV-A or 405 nm laser, either integrated by the manufacturer or added by the end user, can induce DNA damage within the nucleus of a cell and allow the recruitment of DNA repair proteins to the site of induced DNA damage to be monitored. However, as noted in the protocol and representative results, wavelength selection, applied power, and damage characterization are all important issues that must be addressed first by the user in order to study a specific DNA repair pathway. Additionally, there are other considerations in experimental design that must also be considered by users.

In order to monitor a protein's behavior in live cells post micro-irradiation, a fluorescently labeled protein must be created. The availability of a wide range of fluorescent proteins that can be spectrally separated offers tools for creating protein fusions that can be used for characterizing cellular responses to the induction of DNA damage. Transient transfection of fluorescent proteins of interest allows for quick screening of damaging conditions, mutations, or even inhibitors, while stably transfected cells offer more control over expression levels and allow for other biochemical characterizations to be performed, validating micro-irradiation results. Spectrally distinct fluorescent proteins can also be utilized in the same cell to monitor interactions between proteins within the same pathway or in different pathways. Fluorescent proteins also eliminate the need for specific antibodies for each protein of interest and allow live cell monitoring of protein behavior for long periods of time after the induction of damage.

However, the use of fluorescent proteins also has drawbacks. Without genetic backgrounds deficient in the protein(s) of interest, endogenous proteins will compete with the fluorescently tagged proteins. Conjugation of the fluorescent tag to the N or C terminus of the protein may alter protein folding, hinder key protein-protein interactions, or block translocation signals; altering function and potentially impacting recruitment dynamics. These effects have been demonstrated in a number of reports where immunofluorescent staining demonstrated dramatically different recruitment and retention times for endogenous proteins at the damage site²⁸. Use of transient transfection or stable clones can also alter the response observed, typically through variations in protein expression levels. Further, the use of multiple fluorescent proteins in a single experiment may also change the dynamics of recruitment, if protein levels are not equilibrated well or if recruitment of the larger fluorescently-tagged protein blocks the recruitment of other proteins. Finally, fluorescent proteins can act as weak sensitization agents, increasing the formation of reactive oxygen species, and potentially altering the DNA damage mixtures induced^{46,47}. Despite these drawbacks, fluorescent proteins offer a number of distinct advantages in studying DNA repair with micro-irradiation, and if users incorporate appropriate controls, such as the damage characterization described here, they can provide new insight into damage response and protein-protein interactions³.

If live cell imaging is not required, immunofluorescence can be used to monitor the response to induced damage. By fixing cells at specific times post damage induction and staining with

antibodies specific for proteins and lesions of interest, static snapshots of damage induction and the recruitment and retention of repair proteins can be built. Antibodies can be used to monitor the recruitment of multiple proteins of interest and/or post-translational modifications induced by the DNA damage response. Use of immunofluorescence eliminates the need for fluorescent proteins, and allows for endogenous protein behavior to be examined. However, this method too has its drawbacks. Highly specific antibodies are necessary, and permeabilization and blocking procedures need to be optimized to allow for detection of recruitment with sufficient signal intensity. Fixing procedures are not instantaneous, and this physical constraint limits the temporal resolution of this approach. Mapping the site of damage induction so cells can be re-located after staining can also present significant challenges. The confocal microscope used in this work allows for image-based registration as described above, so damaged cells can be relocated with high precision. If stage registration or etched coverglass is not available, the time investment involved in relocating cells without stage registration, coupled with the inherent delay between damage induction and the imaged recruitment, may make immunofluorescence unattractive to some users. However, the most accurate and complete micro-irradiation experimental designs will incorporate these types of approaches in parallel with the use of fluorescent proteins, as described in the presented protocol.

Here, both live cell imaging and immunofluorescence is used to demonstrate the utility of laser micro-irradiation. Immunofluorescent staining allows us to accurately examine the mixture of DNA damage created and the recruitment of proteins induced by each laser power, which allow us to better interpret the observed alterations in the recruitment and retention of XRCC1-GFP. Based on these results, the use of 405 nm lasers should be limited for examination of BER and SSB proteins. Further, the optimal experimental design would include power measurements after the objective, a full damage mixture characterization for each cell line used, and validation of the recruitment and retention observed in fluorescently tagged proteins with immunofluorescence. Obviously, equipment, time, and cost considerations may make these optimal experimental designs impossible for some users. However, the importance of each of these elements is demonstrated here, and users should keep these considerations in mind when beginning micro-irradiation experiments.

ACKNOWLEDGMENTS:

The authors would like to thank Dr. Samuel H. Wilson at the National Institute of Environmental Health Sciences for the cell lines used in this work.

DISCLOSURES:

The authors have nothing to disclose.

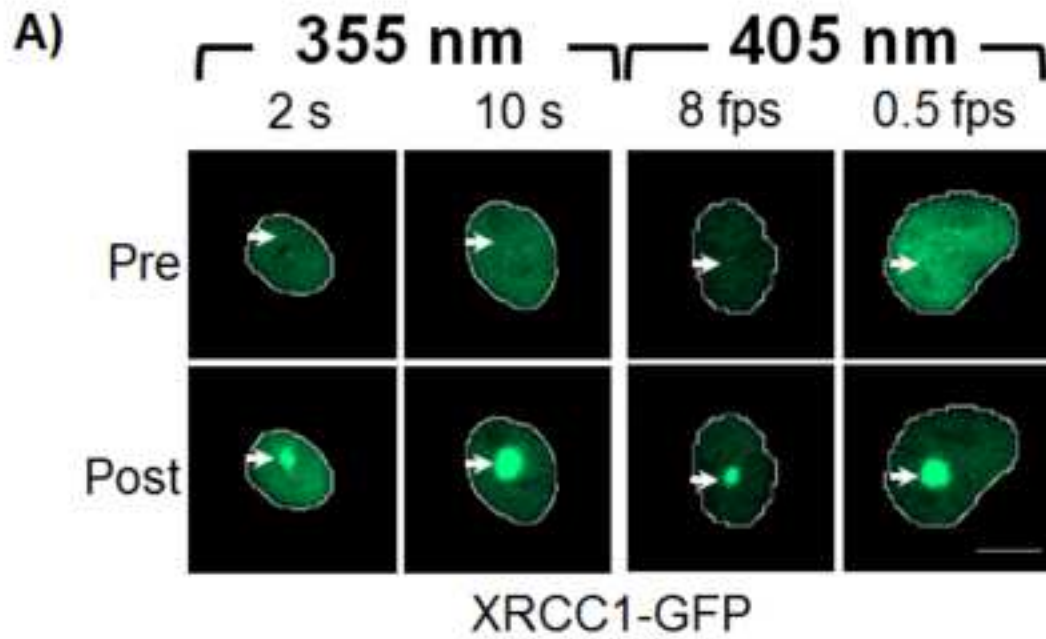
REFERENCES:

- 1 Lijsterburg, M. S. *et al.* Stochastic and reversible assembly of a multiprotein DNA repair complex ensures accurate target site recognition and efficient repair. *J Cell Biol.* **189** (3), 445-463, doi:10.1083/jcb.200909175 (2010).
- 2 Vermeulen, W. Dynamics of mammalian NER proteins. *DNA Repair (Amst).* **10** (7), 760-

- 771, doi:10.1016/j.dnarep.2011.04.015 (2011).
- 3 Berns, M. W. A history of laser scissors (microbeams). *Methods Cell Biol.* **82** 1-58, doi:10.1016/S0091-679X(06)82001-7 (2007).
 - 4 Cremer, C., Cremer, T., Zorn, C. & Schoeller, L. Effects of laser uv-microirradiation ($\lambda = 2573 \text{ \AA}$) on proliferation of Chinese hamster cells. *Radiat Res.* **66** (1), 106-121 (1976).
 - 5 Cremer, C., Cremer, T., Fukuda, M. & Nakanishi, K. Detection of laser--UV microirradiation-induced DNA photolesions by immunofluorescent staining. *Hum Genet.* **54** (1), 107-110 (1980).
 - 6 Walter, J., Cremer, T., Miyagawa, K. & Tashiro, S. A new system for laser-UVA-microirradiation of living cells. *J Microsc.* **209** (Pt 2), 71-75 (2003).
 - 7 Kielbassa, C., Roza, L. & Epe, B. Wavelength dependence of oxidative DNA damage induced by UV and visible light. *Carcinogenesis.* **18** (4), 811-816 (1997).
 - 8 Kielbassa, C. & Epe, B. DNA damage induced by ultraviolet and visible light and its wavelength dependence. *Methods Enzymol.* **319** 436-445 (2000).
 - 9 Kong, X. *et al.* Comparative analysis of different laser systems to study cellular responses to DNA damage in mammalian cells. *Nucleic Acids Res.* **37** (9), e68, doi:10.1093/nar/gkp221 (2009).
 - 10 Lan, L. *et al.* In situ analysis of repair processes for oxidative DNA damage in mammalian cells. *Proc Natl Acad Sci U S A.* **101** (38), 13738-13743, doi:10.1073/pnas.0406048101 (2004).
 - 11 Krasin, F. & Hutchinson, F. Strand breaks and alkali-labile bonds induced by ultraviolet light in DNA with 5-bromouracil in vivo. *Biophys J.* **24** (3), 657-664, doi:10.1016/S0006-3495(78)85411-3 (1978).
 - 12 Krasin, F. & Hutchinson, F. Double-strand breaks from single photochemical events in DNA containing 5-bromouracil. *Biophys J.* **24** (3), 645-656, doi:10.1016/S0006-3495(78)85410-1 (1978).
 - 13 Rosenstein, B. S., Setlow, R. B. & Ahmed, F. E. Use of the dye Hoechst 33258 in a modification of the bromodeoxyuridine photolysis technique for the analysis of DNA repair. *Photochem Photobiol.* **31** (3), 215-222 (1980).
 - 14 Cremer, T., Peterson, S. P., Cremer, C. & Berns, M. W. Laser microirradiation of Chinese hamster cells at wavelength 365 nm: effects of psoralen and caffeine. *Radiat Res.* **85** (3), 529-543 (1981).
 - 15 Limoli, C. L. & Ward, J. F. A new method for introducing double-strand breaks into cellular DNA. *Radiat Res.* **134** (2), 160-169 (1993).
 - 16 Carlsson, K., Mossberg, K., Helm, P. J. & Philip, J. Use of UV excitation in confocal laser scanning fluorescence microscopy. *Micron and Microscopica Acta.* **23** (4), 413-428, doi:10.1016/0739-6260(92)90017-8 (1992).
 - 17 Stelzer, E. H. K. & Haar, F.-M. Confocal Microscopy: Recent Developments. *Advances in Imaging and Electron Physics.* **106** 293-345, doi:10.1016/S1076-5670(08)70273-8 (1999).
 - 18 Rogakou, E. P., Boon, C., Redon, C. & Bonner, W. M. Megabase chromatin domains involved in DNA double-strand breaks in vivo. *J Cell Biol.* **146** (5), 905-916 (1999).
 - 19 Tashiro, S., Walter, J., Shinohara, A., Kamada, N. & Cremer, T. Rad51 accumulation at sites of DNA damage and in postreplicative chromatin. *J Cell Biol.* **150** (2), 283-291

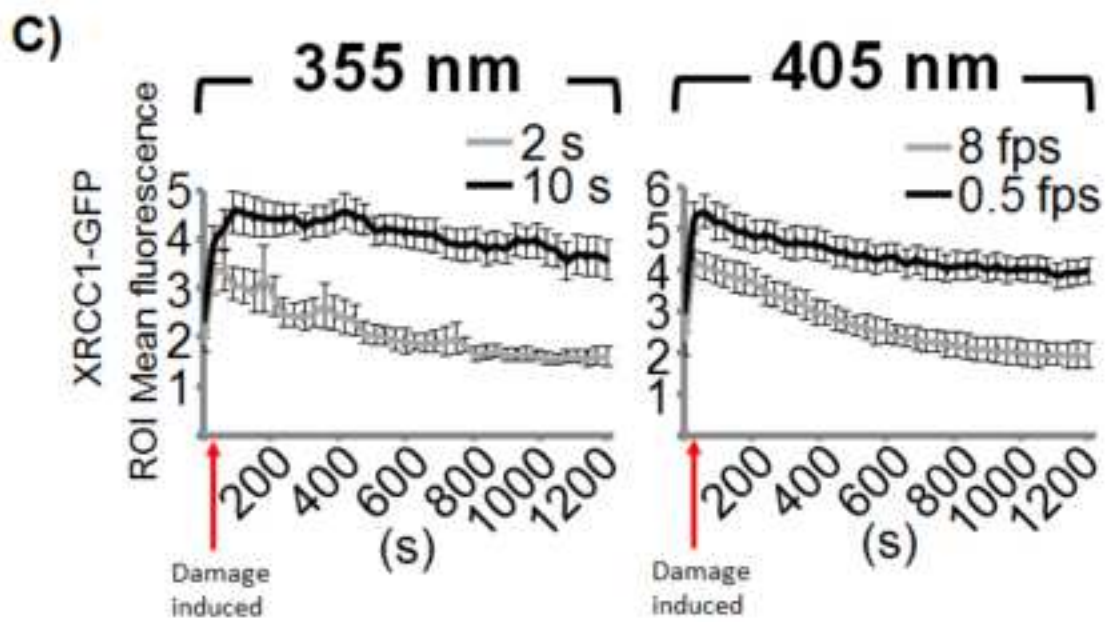
- (2000).
- 20 Gassman, N. R., Stefanick, D. F., Kedar, P. S., Horton, J. K. & Wilson, S. H. Hyperactivation of PARP triggers nonhomologous end-joining in repair-deficient mouse fibroblasts. *PLoS One*. **7** (11), e49301, doi:10.1371/journal.pone.0049301 (2012).
- 21 Bolin, C. *et al.* The impact of cyclin-dependent kinase 5 depletion on poly(ADP-ribose) polymerase activity and responses to radiation. *Cell Mol Life Sci*. **69** (6), 951-962, doi:10.1007/s00018-011-0811-6 (2012).
- 22 Godon, C. *et al.* PARP inhibition versus PARP-1 silencing: different outcomes in terms of single-strand break repair and radiation susceptibility. *Nucleic Acids Res*. **36** (13), 4454-4464, doi:10.1093/nar/gkn403 (2008).
- 23 Hanssen-Bauer, A. *et al.* XRCC1 coordinates disparate responses and multiprotein repair complexes depending on the nature and context of the DNA damage. *Environ Mol Mutagen*. **52** (8), 623-635, doi:10.1002/em.20663 (2011).
- 24 Mortusewicz, O., Amé, J. C., Schreiber, V. & Leonhardt, H. Feedback-regulated poly(ADP-ribosylation) by PARP-1 is required for rapid response to DNA damage in living cells. *Nucleic Acids Res*. **35** (22), 7665-7675, doi:10.1093/nar/gkm933 (2007).
- 25 Mortusewicz, O., Leonhardt, H. & Cardoso, M. C. Spatiotemporal dynamics of regulatory protein recruitment at DNA damage sites. *J Cell Biochem*. **104** (5), 1562-1569, doi:10.1002/jcb.21751 (2008).
- 26 Mortusewicz, O., Rothbauer, U., Cardoso, M. C. & Leonhardt, H. Differential recruitment of DNA Ligase I and III to DNA repair sites. *Nucleic Acids Res*. **34** (12), 3523-3532, doi:10.1093/nar/gkl492 (2006).
- 27 Solarczyk, K. J., Zarębski, M. & Dobrucki, J. W. Inducing local DNA damage by visible light to study chromatin repair. *DNA Repair (Amst)*. **11** (12), 996-1002, doi:10.1016/j.dnarep.2012.09.008 (2012).
- 28 Gassman, N. R. & Wilson, S. H. Micro-irradiation tools to visualize base excision repair and single-strand break repair. *DNA Repair (Amst)*. **31** 52-63, doi:10.1016/j.dnarep.2015.05.001 (2015).
- 29 Botchway, S. W., Reynolds, P., Parker, A. W. & O'Neill, P. Use of near infrared femtosecond lasers as sub-micron radiation microbeam for cell DNA damage and repair studies. *Mutat Res*. **704** (1-3), 38-44, doi:10.1016/j.mrrev.2010.01.003 (2010).
- 30 Ferrando-May, E. *et al.* Highlighting the DNA damage response with ultrashort laser pulses in the near infrared and kinetic modeling. *Front Genet*. **4** 135, doi:10.3389/fgene.2013.00135 (2013).
- 31 Lan, L. *et al.* Accumulation of Werner protein at DNA double-strand breaks in human cells. *J Cell Sci*. **118** (Pt 18), 4153-4162, doi:10.1242/jcs.02544 (2005).
- 32 Salmon, T. B., Evert, B. A., Song, B. & Doetsch, P. W. Biological consequences of oxidative stress-induced DNA damage in *Saccharomyces cerevisiae*. *Nucleic Acids Res*. **32** (12), 3712-3723, doi:10.1093/nar/gkh696 (2004).
- 33 Caldecott, K. W. DNA single-strand break repair. *Exp Cell Res*. **329** (1), 2-8, doi:10.1016/j.yexcr.2014.08.027 (2014).
- 34 London, R. E. The structural basis of XRCC1-mediated DNA repair. *DNA Repair (Amst)*. **30** 90-103, doi:10.1016/j.dnarep.2015.02.005 (2015).
- 35 Moser, J. *et al.* Sealing of chromosomal DNA nicks during nucleotide excision repair

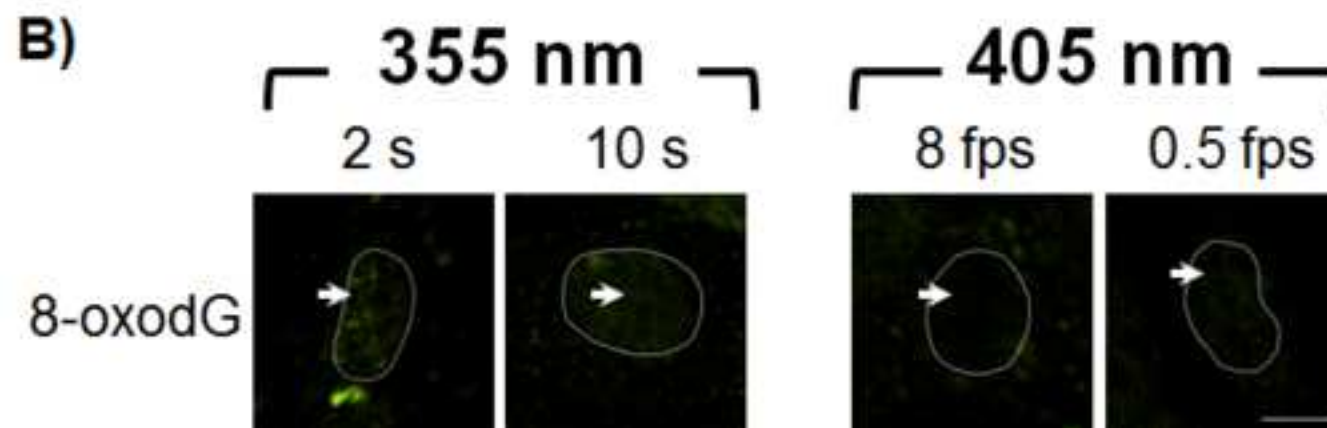
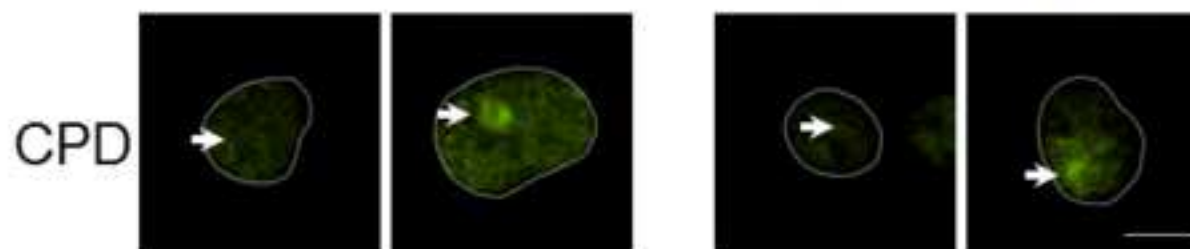
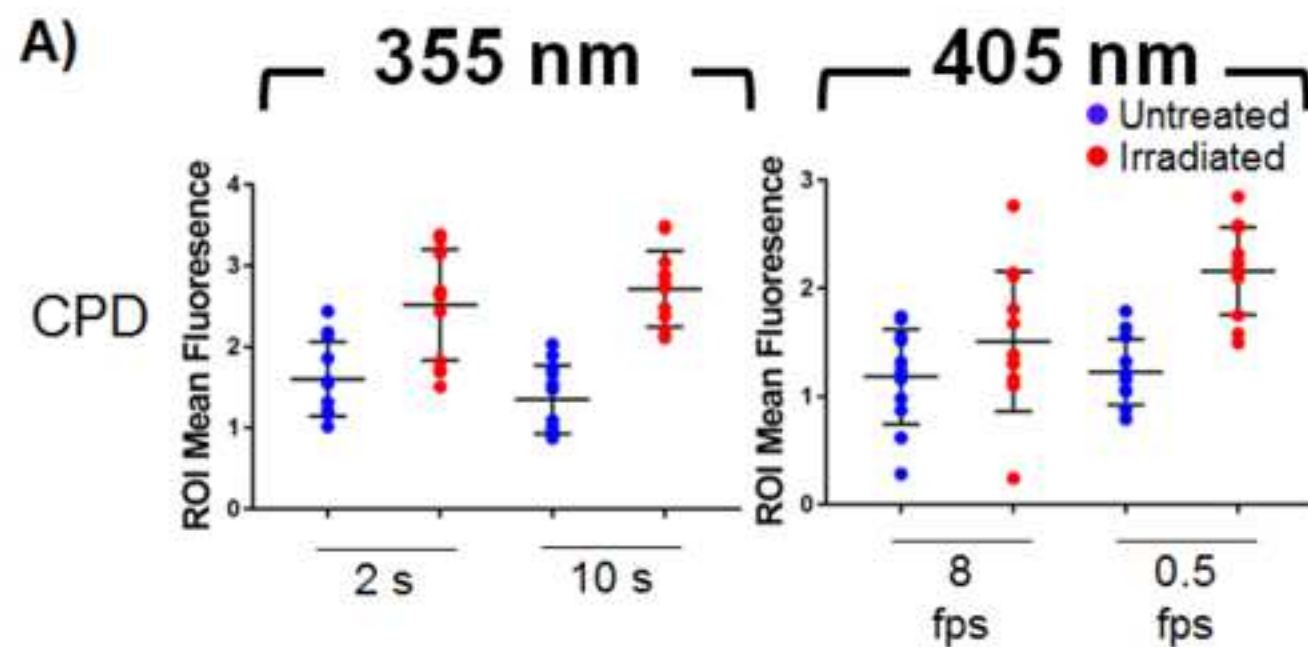
- requires XRCC1 and DNA ligase III alpha in a cell-cycle-specific manner. *Mol Cell*. **27** (2), 311-323, doi:10.1016/j.molcel.2007.06.014 (2007).
- 36 Campalans, A. *et al.* Distinct spatiotemporal patterns and PARP dependence of XRCC1 recruitment to single-strand break and base excision repair. *Nucleic Acids Res*. **41** (5), 3115-3129, doi:10.1093/nar/gkt025 (2013).
- 37 Cooke, M. S. & Lunec, J. *Immunochemical detection of oxidative DNA damage*. Vol. I 275-293 (World Scientific, 2003).
- 38 Rossner, P., Jr. & Sram, R. J. Immunochemical detection of oxidatively damaged DNA. *Free Radic Res*. **46** (4), 492-522, doi:10.3109/10715762.2011.632415 (2012).
- 39 Cleaver, J. E., Feeney, L. & Revet, I. Phosphorylated H2Ax is not an unambiguous marker for DNA double-strand breaks. *Cell Cycle*. **10** (19), 3223-3224, doi:10.4161/cc.10.19.17448 (2011).
- 40 Rybak, P. *et al.* Low level phosphorylation of histone H2AX on serine 139 (γH2AX) is not associated with DNA double-strand breaks. *Oncotarget*. **7** (31), 49574-49587, doi:10.18632/oncotarget.10411 (2016).
- 41 Haince, J. F. *et al.* PARP1-dependent kinetics of recruitment of MRE11 and NBS1 proteins to multiple DNA damage sites. *J Biol Chem*. **283** (2), 1197-1208, doi:10.1074/jbc.M706734200 (2008).
- 42 Caldecott, K. W. Single-strand break repair and genetic disease. *Nat Rev Genet*. **9** (8), 619-631, doi:10.1038/nrg2380 (2008).
- 43 Lomax, M. E., Gulston, M. K. & O'Neill, P. Chemical aspects of clustered DNA damage induction by ionising radiation. *Radiat Prot Dosimetry*. **99** (1-4), 63-68 (2002).
- 44 Ma, W., Westmoreland, J. W., Gordenin, D. A. & Resnick, M. A. Alkylation base damage is converted into repairable double-strand breaks and complex intermediates in G2 cells lacking AP endonuclease. *PLoS Genet*. **7** (4), e1002059, doi:10.1371/journal.pgen.1002059 (2011).
- 45 Siddiqi, M. A. & Bothe, E. Single- and double-strand break formation in DNA irradiated in aqueous solution: dependence on dose and OH radical scavenger concentration. *Radiat Res*. **112** (3), 449-463 (1987).
- 46 Sano, Y., Watanabe, W. & Matsunaga, S. Chromophore-assisted laser inactivation--towards a spatiotemporal-functional analysis of proteins, and the ablation of chromatin, organelle and cell function. *J Cell Sci*. **127** (Pt 8), 1621-1629, doi:10.1242/jcs.144527 (2014).
- 47 Wojtovich, A. P. & Foster, T. H. Optogenetic control of ROS production. *Redox Biol*. **2** 368-376, doi:10.1016/j.redox.2014.01.019 (2014).

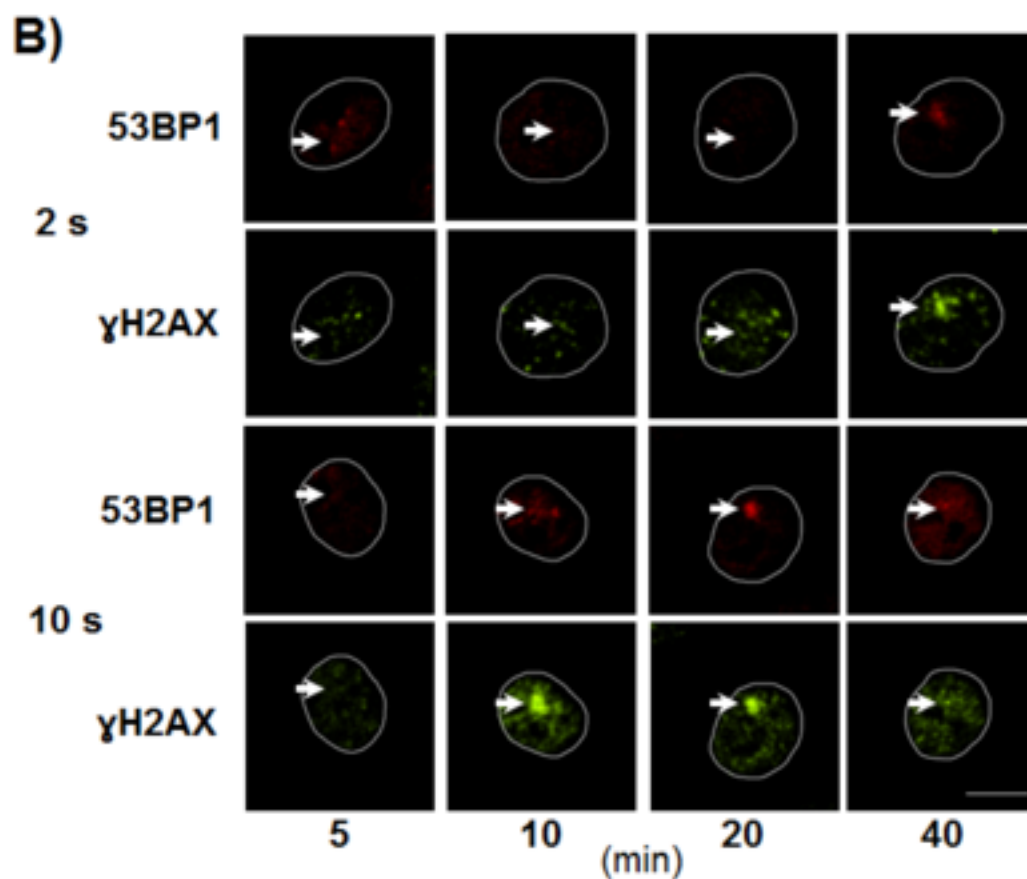
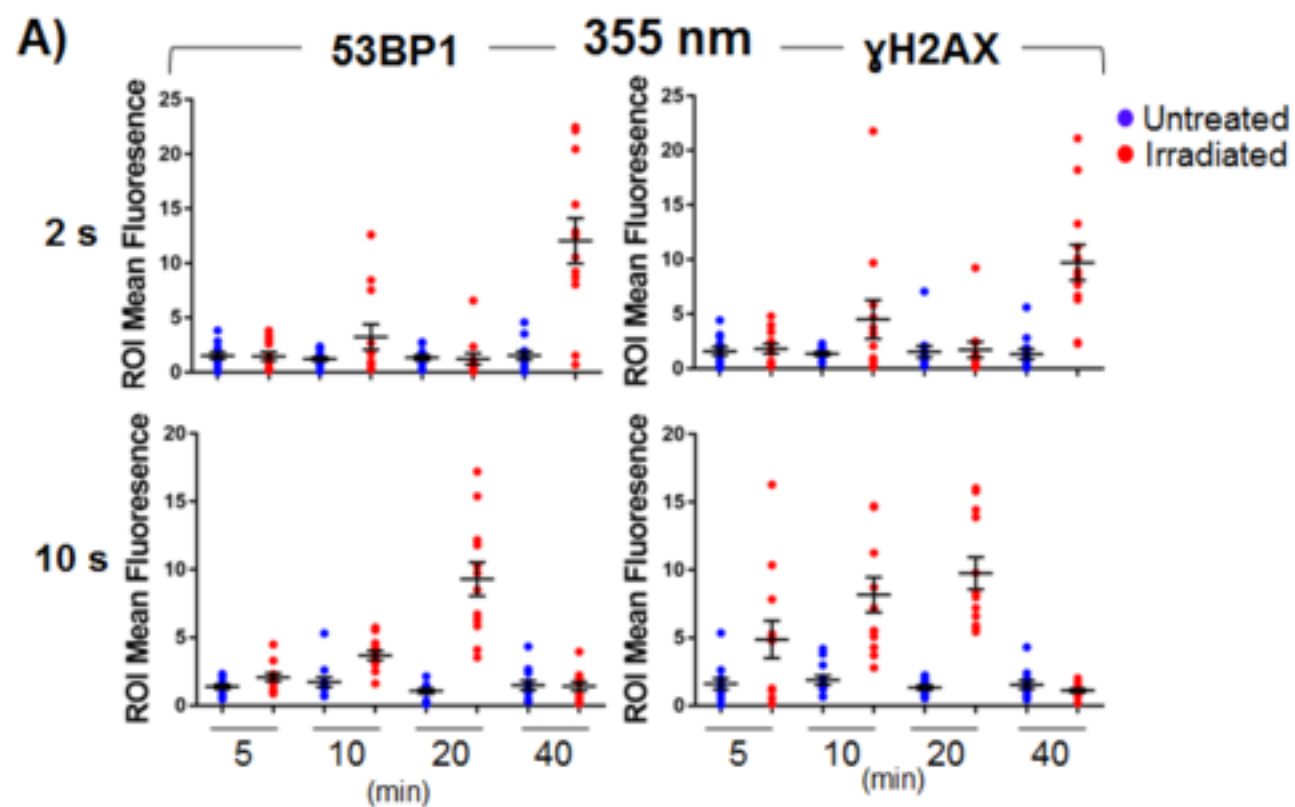


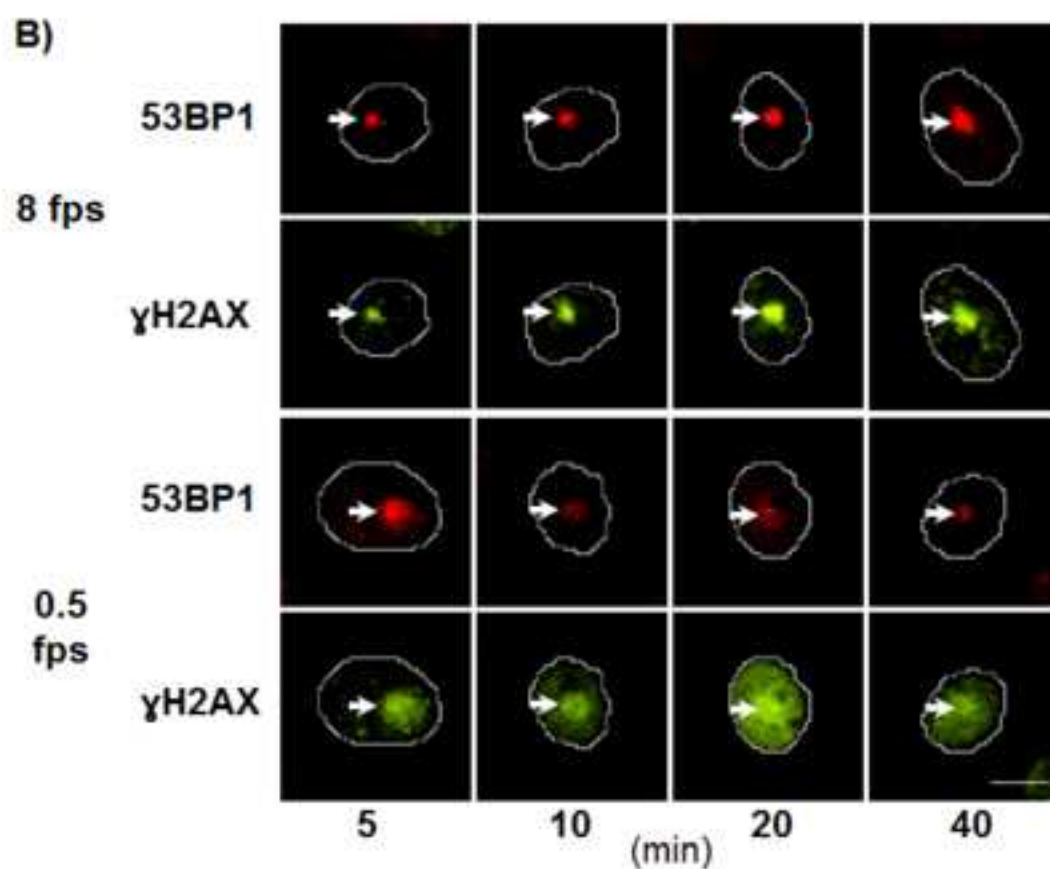
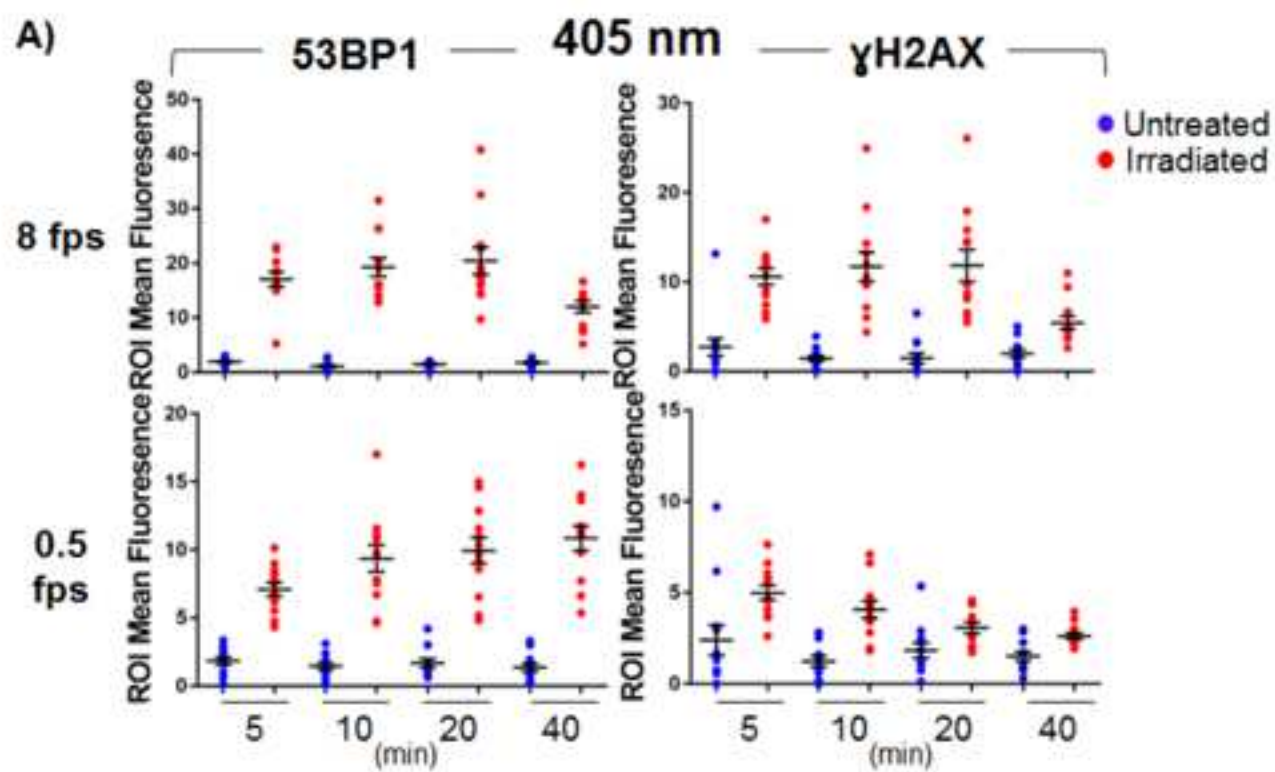
B)

$$\text{ROI Mean Fluorescence Intensity} = \frac{\text{Damage ROI}}{\text{Nucleus}}$$









Name of Material/ Equipment	Company	Catalog Number	Comments/Description
Nikon A1rsi laser scanning confocal microscope	Nikon		
NIS Elements software	Nikon		
355 nm laser	PicoQuant VisUV		Radiation source
Galvanometer photoactivation miniscanner	Bruker		
Microscope slide photodiode power sensor	THORLabs	S170C	
Fiber photodiode power sensor	THORLabs	S150C	
Digital handheld optical power and energy	THORLabs	PM100D	
CHO-K1			From Dr. Samuel H. Wilson, NIEHS
Minimal essential media	Hyclone	SH3026501	
Fetal bovine serum	Atlanta biologicals	S11550	
XRCC1-GFP	Origene	RG204952	
Jetprime	Polyplus transfection	11407	
Geneticin	ThermoFisher	10131035	
4 chambered coverglass	ThermoFisher	155382	
8 chambered coverglass	ThermoFisher	155409	
Anti 53BP-1	Novus	NB100304	
Anti-phospho-histone H2AX	Millipore	05-636-I	
Anti cyclobutane pyrimidine dimer	Cosmo Bio clone	CAC-NM-DND-	
Anti 8-oxo-2'-deoxyguanosine	Trevigen	4354-MC-050	
Alexa 488 goat anti-mouse	ThermoFisher	A11029	
Alexa 546 goat anti-rabbit	ThermoFisher	A11010	
4',6-Diamidino-2-Phenylindole (DAPI)	ThermoFisher	R37606	Caution toxic!
Phosphate buffered saline	ThermoFisher	0780	
Normal goat serum	ThermoFisher	31873	
Bovine serum albumin (BSA)	Jackson Immuno	001-000-162	
37% Formaldehyde	ThermoFisher	9311	Caution toxic!
Ethanol	Decon Labs	2716	
Methanol	VWR	BDH1135	Caution toxic!
HCl	Fisher	SA49	
Sodium azide	Sigma-Aldrich	S2002	Caution toxic!
Tris Hydrochloride	Amresco	O234	
Triton X-100	Sigma-Aldrich	T8787	



1 Alewife Center #200
Cambridge, MA 02140
tel. 617.945.9051
www.jove.com

ARTICLE AND VIDEO LICENSE AGREEMENT

Title of Article:

Author(s):

Item 1 (check one box): The Author elects to have the Materials be made available (as described at <http://www.jove.com/author>) via: ☒ Standard Access ☐ Open Access

Item 2 (check one box):

- ☒ The Author is NOT a United States government employee.
- ☐ The Author is a United States government employee and the Materials were prepared in the course of his or her duties as a United States government employee.
- ☐ The Author is a United States government employee but the Materials were NOT prepared in the course of his or her duties as a United States government employee.

ARTICLE AND VIDEO LICENSE AGREEMENT

1. Defined Terms. As used in this Article and Video License Agreement, the following terms shall have the following meanings: “**Agreement**” means this Article and Video License Agreement; “**Article**” means the article specified on the last page of this Agreement, including any associated materials such as texts, figures, tables, artwork, abstracts, or summaries contained therein; “**Author**” means the author who is a signatory to this Agreement; “**Collective Work**” means a work, such as a periodical issue, anthology or encyclopedia, in which the Materials in their entirety in unmodified form, along with a number of other contributions, constituting separate and independent works in themselves, are assembled into a collective whole; “**CRC License**” means the Creative Commons Attribution-Non Commercial-No Derivs 3.0 Unported Agreement, the terms and conditions of which can be found at: <http://creativecommons.org/licenses/by-nc-nd/3.0/legalcode>; “**Derivative Work**” means a work based upon the Materials or upon the Materials and other pre-existing works, such as a translation, musical arrangement, dramatization, fictionalization, motion picture version, sound recording, art reproduction, abridgment, condensation, or any other form in which the Materials may be recast, transformed, or adapted; “**Institution**” means the institution, listed on the last page of this Agreement, by which the Author was employed at the time of the creation of the Materials; “**JoVE**” means MyJoVE Corporation, a Massachusetts corporation and the publisher of *The Journal of Visualized Experiments*; “**Materials**” means the Article and / or the Video; “**Parties**” means the Author and JoVE; “**Video**” means any video(s) made by the Author, alone or in conjunction with any other parties, or by JoVE or its affiliates or agents, individually or in collaboration with the Author or any other parties, incorporating all or any portion of the Article, and in which the Author may or may not appear.

2. Background. The Author, who is the author of the Article, in order to ensure the dissemination and protection of the Article, desires to have the JoVE publish the Article and create and transmit videos based on the Article. In furtherance of such goals, the Parties desire to memorialize in this Agreement the respective rights of each Party in and to the Article and the Video.

3. Grant of Rights in Article. In consideration of JoVE agreeing to publish the Article, the Author hereby grants to JoVE, subject to **Sections 4** and **7** below, the exclusive, royalty-free, perpetual (for the full term of copyright in the Article, including any extensions thereto) license (a) to publish, reproduce, distribute, display and store the Article in all forms, formats and media whether now known or hereafter developed (including without limitation in print, digital and electronic form) throughout the world, (b) to translate the Article into other languages, create adaptations, summaries or extracts of the Article or other Derivative Works (including, without limitation, the Video) or Collective Works based on all or any portion of the Article and exercise all of the rights set forth in (a) above in such translations, adaptations, summaries, extracts, Derivative Works or Collective Works and (c) to license others to do any or all of the above. The foregoing rights may be exercised in all media and formats, whether now known or hereafter devised, and include the right to make such modifications as are technically necessary to exercise the rights in other media and formats. If the “Open Access” box has been checked in **Item 1** above, JoVE and the Author hereby grant to the public all such rights in the Article as provided in, but subject to all limitations and requirements set forth in, the CRC License.

ARTICLE AND VIDEO LICENSE AGREEMENT

4. Retention of Rights in Article. Notwithstanding the exclusive license granted to JoVE in **Section 3** above, the Author shall, with respect to the Article, retain the non-exclusive right to use all or part of the Article for the non-commercial purpose of giving lectures, presentations or teaching classes, and to post a copy of the Article on the Institution's website or the Author's personal website, in each case provided that a link to the Article on the JoVE website is provided and notice of JoVE's copyright in the Article is included. All non-copyright intellectual property rights in and to the Article, such as patent rights, shall remain with the Author.

5. Grant of Rights in Video – Standard Access. This **Section 5** applies if the "Standard Access" box has been checked in **Item 1** above or if no box has been checked in **Item 1** above. In consideration of JoVE agreeing to produce, display or otherwise assist with the Video, the Author hereby acknowledges and agrees that, Subject to **Section 7** below, JoVE is and shall be the sole and exclusive owner of all rights of any nature, including, without limitation, all copyrights, in and to the Video. To the extent that, by law, the Author is deemed, now or at any time in the future, to have any rights of any nature in or to the Video, the Author hereby disclaims all such rights and transfers all such rights to JoVE.

6. Grant of Rights in Video – Open Access. This **Section 6** applies only if the "Open Access" box has been checked in **Item 1** above. In consideration of JoVE agreeing to produce, display or otherwise assist with the Video, the Author hereby grants to JoVE, subject to **Section 7** below, the exclusive, royalty-free, perpetual (for the full term of copyright in the Article, including any extensions thereto) license (a) to publish, reproduce, distribute, display and store the Video in all forms, formats and media whether now known or hereafter developed (including without limitation in print, digital and electronic form) throughout the world, (b) to translate the Video into other languages, create adaptations, summaries or extracts of the Video or other Derivative Works or Collective Works based on all or any portion of the Video and exercise all of the rights set forth in (a) above in such translations, adaptations, summaries, extracts, Derivative Works or Collective Works and (c) to license others to do any or all of the above. The foregoing rights may be exercised in all media and formats, whether now known or hereafter devised, and include the right to make such modifications as are technically necessary to exercise the rights in other media and formats. For any Video to which this Section 6 is applicable, JoVE and the Author hereby grant to the public all such rights in the Video as provided in, but subject to all limitations and requirements set forth in, the CRC License.

7. Government Employees. If the Author is a United States government employee and the Article was prepared in the course of his or her duties as a United States government employee, as indicated in **Item 2** above, and any of the licenses or grants granted by the Author hereunder exceed the scope of the 17 U.S.C. 403, then the rights granted hereunder shall be limited to the maximum rights permitted under such

statute. In such case, all provisions contained herein that are not in conflict with such statute shall remain in full force and effect, and all provisions contained herein that do so conflict shall be deemed to be amended so as to provide to JoVE the maximum rights permissible within such statute.

8. Likeness, Privacy, Personality. The Author hereby grants JoVE the right to use the Author's name, voice, likeness, picture, photograph, image, biography and performance in any way, commercial or otherwise, in connection with the Materials and the sale, promotion and distribution thereof. The Author hereby waives any and all rights he or she may have, relating to his or her appearance in the Video or otherwise relating to the Materials, under all applicable privacy, likeness, personality or similar laws.

9. Author Warranties. The Author represents and warrants that the Article is original, that it has not been published, that the copyright interest is owned by the Author (or, if more than one author is listed at the beginning of this Agreement, by such authors collectively) and has not been assigned, licensed, or otherwise transferred to any other party. The Author represents and warrants that the author(s) listed at the top of this Agreement are the only authors of the Materials. If more than one author is listed at the top of this Agreement and if any such author has not entered into a separate Article and Video License Agreement with JoVE relating to the Materials, the Author represents and warrants that the Author has been authorized by each of the other such authors to execute this Agreement on his or her behalf and to bind him or her with respect to the terms of this Agreement as if each of them had been a party hereto as an Author. The Author warrants that the use, reproduction, distribution, public or private performance or display, and/or modification of all or any portion of the Materials does not and will not violate, infringe and/or misappropriate the patent, trademark, intellectual property or other rights of any third party. The Author represents and warrants that it has and will continue to comply with all government, institutional and other regulations, including, without limitation all institutional, laboratory, hospital, ethical, human and animal treatment, privacy, and all other rules, regulations, laws, procedures or guidelines, applicable to the Materials, and that all research involving human and animal subjects has been approved by the Author's relevant institutional review board.

10. JoVE Discretion. If the Author requests the assistance of JoVE in producing the Video in the Author's facility, the Author shall ensure that the presence of JoVE employees, agents or independent contractors is in accordance with the relevant regulations of the Author's institution. If more than one author is listed at the beginning of this Agreement, JoVE may, in its sole discretion, elect not take any action with respect to the Article until such time as it has received complete, executed Article and Video License Agreements from each such author. JoVE reserves the right, in its absolute and sole discretion and without giving any reason therefore, to accept or decline any work submitted to JoVE. JoVE and its employees, agents and independent contractors shall have

ARTICLE AND VIDEO LICENSE AGREEMENT

full, unfettered access to the facilities of the Author or of the Author's institution as necessary to make the Video, whether actually published or not. JoVE has sole discretion as to the method of making and publishing the Materials, including, without limitation, to all decisions regarding editing, lighting, filming, timing of publication, if any, length, quality, content and the like.

11. **Indemnification.** The Author agrees to indemnify JoVE and/or its successors and assigns from and against any and all claims, costs, and expenses, including attorney's fees, arising out of any breach of any warranty or other representations contained herein. The Author further agrees to indemnify and hold harmless JoVE from and against any and all claims, costs, and expenses, including attorney's fees, resulting from the breach by the Author of any representation or warranty contained herein or from allegations or instances of violation of intellectual property rights, damage to the Author's or the Author's institution's facilities, fraud, libel, defamation, research, equipment, experiments, property damage, personal injury, violations of institutional, laboratory, hospital, ethical, human and animal treatment, privacy or other rules, regulations, laws, procedures or guidelines, liabilities and other losses or damages related in any way to the submission of work to JoVE, making of videos by JoVE, or publication in JoVE or elsewhere by JoVE. The Author shall be responsible for, and shall hold JoVE harmless from, damages caused by lack of sterilization, lack of cleanliness or by contamination due to the making of a video by JoVE its employees, agents or independent contractors. All sterilization, cleanliness or decontamination procedures shall be solely the responsibility of the Author and shall be undertaken at the Author's


expense. All indemnifications provided herein shall include JoVE's attorney's fees and costs related to said losses or damages. Such indemnification and holding harmless shall include such losses or damages incurred by, or in connection with, acts or omissions of JoVE, its employees, agents or independent contractors.

12. **Fees.** To cover the cost incurred for publication, JoVE must receive payment before production and publication the Materials. Payment is due in 21 days of invoice. Should the Materials not be published due to an editorial or production decision, these funds will be returned to the Author. Withdrawal by the Author of any submitted Materials after final peer review approval will result in a US\$1,200 fee to cover pre-production expenses incurred by JoVE. If payment is not received by the completion of filming, production and publication of the Materials will be suspended until payment is received.

13. **Transfer, Governing Law.** This Agreement may be assigned by JoVE and shall inure to the benefits of any of JoVE's successors and assignees. This Agreement shall be governed and construed by the internal laws of the Commonwealth of Massachusetts without giving effect to any conflict of law provision thereunder. This Agreement may be executed in counterparts, each of which shall be deemed an original, but all of which together shall be deemed to be one and the same agreement. A signed copy of this Agreement delivered by facsimile, e-mail or other means of electronic transmission shall be deemed to have the same legal effect as delivery of an original signed copy of this Agreement.

A signed copy of this document must be sent with all new submissions. Only one Agreement required per submission.

CORRESPONDING AUTHOR:

Name:	Natalie R. Gassman	
Department:	Oncologic Sciences	
Institution:	University of South Alabama Mitchell Cancer Institute	
Article Title:	Application of laser micro-irradiation for examination of single and double strand break repair in cells	
Signature:		Date: 3/8/17

Please submit a signed and dated copy of this license by one of the following three methods:

- 1) Upload a scanned copy of the document as a pdf on the JoVE submission site;
- 2) Fax the document to +1.866.381.2236;
- 3) Mail the document to JoVE / Attn: JoVE Editorial / 1 Alewife Center #200 / Cambridge, MA 02139

For questions, please email submissions@jove.com or call +1.617.945.9051



Dr. Nguyen,

Enclosed is our revised manuscript "Application of laser micro-irradiation for examination of single and double strand break repair in mammalian cells." We would like to thank the reviewers for their helpful comments, and in this revision, we have addressed their concerns as thoroughly as possible. As noted by the editor, all of the reviews noted a major concern with the description of the technique and its general applicability to the study of DNA damage. We agree with a number of the comments made by the reviewers addressing the utility of the method for studying single strand breaks specifically, the generalizability of the method to a number of microscopes, and the inherent difficulties presented by using 405 nm wavelengths. However, the goal of this article is to provide individuals with a protocol for broadly applying micro-irradiation to their studies. There are numerous reviews that highlight and discuss the issues raised by the reviewers, and we have cited them throughout the manuscript. Since micro-irradiation is being employed more frequently in the assessment of DNA damage response and repair, we sought to develop a general protocol that addresses the wavelengths commonly used in the literature and highlight some necessary characterization and quantification procedures that are frequently lacking in current reports. With this goal in mind, we designed a protocol to allow any user with a microscope to employ micro-irradiation experiments. Like other JoVE articles, it is a guide to help new users develop and employ this technique and a reference for experienced users to update and expand their current protocols. There are inherent limitations into what we could include and still make the method: a) generalizable and b) practical. With this in mind, we have sought to address as many of the issues raised by the reviewers as possible, and hope that this article can help bring more users to micro-irradiation and spawn further protocols that address and refine the method.

Below we have addressed the comments made by each reviewer.

Editorial comments: **We have re-read the final version and addressed the issues mentioned here.**

Changes to be made by the Author(s):

1. Please take this opportunity to thoroughly proofread the manuscript to ensure that there are no spelling or grammar issues. The JoVE editor will not copy-edit your manuscript and any errors in the submitted revision may be present in the published version.
2. Please define all abbreviations before use.
3. Please use SI abbreviations for time in the manuscript and the Figures: h, min, s

Reviewer #1:

Major Concerns:

At step 3.3 more emphasis should be given to the point of finding the right z-focus. This is crucial to achieve a proper response and is not trivial, in particular if the cells are not labelled with a fluorescent marker.

We have included a procedure to help users better define the focal plane within which the micro-irradiation is to occur. This method is described for both the fluorescently labeled and unlabeled cells in Section 3.3 and will be included in the video. See lines 197-206.

1660 Springhill Avenue
Mobile, AL 36604-1405

Tel: (251) 460-6993
Fax: (251) 460-6994

Comprehensive Oncology Healthcare & Research



At step 3.5.1.2 the authors should discuss how many cells they recommend to irradiate and give some guidelines about the experimental repeats need to yield robust results in their experience.

We have included additional recommendations for the number of cells and suggestions for making the experimental results more robust. Lines 259-266.

The immunofluorescence protocol is clearly explained and can be easily followed step by step. The antibody used for labelling 8-oxo-dG is known to give very poor results. It is not surprising that the authors do not detect any signal using this antibody. Oxidative base damage is very likely if not certain to occur as a consequence of laser microirradiation at the indicated wavelengths. The absence of signal is due to the poor performance of the antibody and should not be interpreted as a lack of oxidative base damage.

We agree with the reviewer that antibody specificity can be significant issue in the detection and quantification of DNA adduct formation. However, the procedure and the antibody clone used have been successful in a number of publications (Lan, Nakajima et al. 2004, Kong, Mohanty et al. 2009, Campalans, Moritz et al. 2015). To better address this issue we have included language stating that when possible, two markers for strand breaks or base lesions should be employed. In the case of 8-oxodG, we also mention that recruitment of OGG1 can be used as a marker, previously cited by Lan, Nakajima et al. 2004.

In our case, we do not observed the recruitment of OGG1 to the low dose power, and we believe the induction of oxidatively induced base lesion is low, which is comparable to the Lan et al. work. Lines 533-542.

The results section should also present an image of the γ H2AX immunostaining at high and low doses, since high doses can possibly lead to a pan-nuclear staining that should be avoided. Users should be made aware of this point.

We have now included additional figures for the γ H2AX staining so the user can better evaluate the signal observed, and we have included high dose pan nuclear staining examples as well. See Figure 4.

The image analysis chapter gives the necessary basic information to approach quantitative evaluation of the image data. While the described procedures can be useful for a researcher approaching for the first time laser microirradiation and needs to understand the practical steps involved, the technique, as it is described here, harbors a fundamental limitation. This consists in the very poor damage selectivity of the wavelengths used for irradiation, in particular 405 nm. The usefulness of the laser microirradiation approach depends crucially on the ability to induce only one and not many different types of DNA damage in order to enable the investigation of individual repair pathways. There is no such "correct DNA damage mixture" (line 381), as the authors propose. A mixed and complex DNA damage will trigger multiple pathways simultaneously and possibly artificially induce cross-talk between them which has no relevance with regard to the physiological response to DNA damage. In fact, this is the major point of criticism with which microirradiation approaches are confronted as compared to other methods introducing strand breaks at selected genomic loci (e.g. Scel-nuclease method). So far the best damage selectivity has been achieved using focused UV-C irradiation (266 nm) for

1660 Springhill Avenue
Mobile, AL 36604-1405

Tel: (251) 460-6993
Fax: (251) 460-6994

Comprehensive Oncology Healthcare & Research



inducing CPDs (see e.g. Dinant et al., 2007) and UV-A (337 nm) in combination with BrdU (see e.g. Lukas et al., 2003). Irradiation at 405 nm induces DSBs among other types of DNA damage. Although very convenient, because a 405 nm diode is provided with most confocal microscopes, the use of this wavelength for DNA repair studies should not be encouraged in my opinion. It is not sufficient to emphasize that the damage spectrum is dose and context dependent and should be thoroughly examined, as the authors repeatedly do. The title and the abstract may thus also lead to wrong interpretations or expectations. The authors do not propose a method to "examine repair of single and double strand breaks". There is no quantitative comparison which would support the notion that oxidative and UV damage are not induced at the same time under the applied conditions. For all these reason, this referee concludes that the manuscript in its present form is not suitable for publication in JoVE. Taken together, I suggest to prepare a new manuscript focusing more on the technical details (coupling of the external laser, options for additional scanner etc.) and showing the influence of irradiation parameters (laser intensity, pixel dwell time, type of objective etc.) on one general damage marker, e.g. recruitment of XRCC1-GFP, without showing any result addressing the damage specificity and omitting the 405 laser line.

The reviewer makes an extremely valid and important point about the nature of the DNA damage induced. Unless a researcher absolutely limits the induction of DNA damage to a single site through host cell reactivation or endonuclease methods, all DNA damaging chemicals create a mixture of DNA damage, which are addressed by a number of DNA repair pathways, many with overlapping substrate specificity. Hydrogen peroxide is the classic example of a reagent that induces a broad spectrum of DNA damage. Additionally, agents like MMS, which primarily induce alkylating DNA damage, has also been shown to induce reactive oxygen species and a mixture of base lesions and single strand breaks. It is fallacy to assume that single types of DNA damage are being generated, though in the micro-irradiation field this fact needs to be more clearly addressed, and we agree with the reviewer on this point. However, the DNA repair field often attempts to generate a preponderance of a single type of DNA damage over others to generalize the behavior of a specific DNA repair protein or DNA repair pathway, and we believe that using the protocol we have developed and the considerations we include that a preponderance of a specific type of DNA damage can be created with micro-irradiation, i.e., a higher ratio of single strand breaks than double strand breaks.

With the exception of 266 nm, which can be directly absorbed by the DNA, all of the UV-B and UV-A wavelengths have the potential to create mixtures of DNA damage the users need to be aware of and acknowledge, and these have been characterized by a number of publications (Kielbassa, Roza et al. 1997, Kielbassa and Epe 2000). However, there is still inherent value in examining how DNA repair proteins react to these damage mixtures, just like there is value in applying an agent like MMS or H₂O₂ to cells and doing immunofluorescence to examine DNA repair protein behavior. While the reviewer's suggestions of a separate paper that characterize specific DNA damage mixtures is valid, the technical requirements and protocols required would be beyond most users. We believe the article and protocol presented offers the best of both worlds, an applicable and implementable technique for a wide array of users that acknowledges the inherent limitations of 405 nm and damage characterization.



We agree that some of the language used in the manuscript appears to indicate that a single type of damage mixture can be obtained with these wavelength, and it may not strongly discourage the use of 405 nm. Therefore, we have reworded and added sections to the manuscript to make this a more central consideration for users. Additionally, we would note that the title does state "single and double strand breaks," which does not imply these repair events can be separated in the least. It indicates the paper gives methods for studying these pathways, which it clearly does.

Minor Concerns:

Line 55: "site-specific": laser microirradiation is spatially selective but not site-specific. Site-specific are damaging techniques that target specific genomic sites.

We have revised the language in this section to address the reviewer's concern.

Line 104-106: "If properly applied...": this sentence is misleading. The generation of "specific mixtures" of DNA damage has not been demonstrated so far and is also almost impossible to achieve in a quantitatively measurable manner, as the statement suggests. Laser micro-irradiation, in particular at 405 nm will generate complex DNA damage which is difficult to characterize because of the limitation of the analytical tools. The authors show no assay how to discriminate between SSB and DSBs, for example. This adds to the general statement made above about the disadvantages of mixed damage induction methods. Importantly, the title of the manuscript should be changed (see above)

As noted in the previous section, we have revised and refined the language in this section and others to address the reviewer's concerns.

Line 126-129: galvanometer should read galvanometer; "NIS-Elements" should be explained

We have made these additions.

Line 141: pinhole set to "69 μm ": this figure is strange. I guess that the authors propose to image with an open pinhole. The actual "size" may differ between different imaging systems.

We have revised to specify the wavelength and airy unit used, since this is standard for most microscopes and will be applicable to numerous microscope configurations.

Line 149: the sentence should read: ..return the cells to an incubator at 37 oC and 5% CO2

We have made this correction.

Line 195: "fluorescent focus": using the term "focus" for the microirradiated ROI is misleading in this context. The term focus refers to the focus of the lens, the focal plan etc. Replace focus with "damaged ROI" or similar term (see also lines

331, 378, 389 , 394)

While focus and foci are the commonly used terminology in the literature, we agree this may be confusing to the reader, so we have revised these sections to “damage ROI.”

Line 381: "ensure that the correct DNA damage mixture is being created for the repair pathway of interest". This is also misleading (see general comments above). The same applies for line 394. The goal should be to generate specific damage and not mixtures which can hardly be characterized, let alone be controlled.

As noted in the previous section, we have revised and refined the language in this section and others to address the reviewer's concerns.

Line 516 posttranslational modification

We have made this correction.

Reviewer #2:

1. The authors seem to describe a mixture of damage types created by their procedure as a desired and expected phenomenon. It is neither desired nor necessary. Low doses of UV are expected to induce typical damage resulting from direct absorption of UV by DNA only. This is useful in studies of NER (Dinant C, de Jager M, Essers J, van Cappellen WA, Kanaar R, Houtsmuller AB, Vermeulen W. J Cell Sci. 2007 Aug 1;120(Pt 15):2731-40. Activation of multiple DNA repair pathways by sub-nuclear damage induction methods, and other papers by this group, using low power UV). However, higher doses of UV presumably act by multiple mechanisms and result not only in typical UV damage but DNA breaks as well. This is unwanted. How can a researcher provide new insights into the mechanism of any repair pathway if several major pathways are activated in the same area at the same time? This way of thinking presented by the authors is confusing and not useful for the inexperienced users of the method described in the submitted paper.

As noted by the other reviewers, a mixture of DNA damage is generated by the UV-A wavelength, and we have revised the language of the manuscript to better reflect this outcome. Please see our comments to Reviewer 1. Additionally, we have clarified the introduction using the reviewer's suggestions.

2. The following statement the authors make is quite surprising in view of the existing knowledge: "These limitations were soon overcome through the incorporation of sensitizing agents, like psoralen, bromodeoxyuridine (BrdU), and Hoechst dyes, which lowered the required laser energy input and expanded the useable wavelengths for damage induction." (line 64-67). The authors refer to the fact that the UV damage (PPs and CPDs) induced by the method described by Cremer brothers and their collaborators was not accompanied by DNA breaks. The authors consider it as a limitation that needed

to be overcome. It is the other way around. The goal should be to induce one type of damage, moreover to keep it at a low level, in order to study the reaction of a cell in a relevant way (Bekker-Jensen S, Lukas C, Kitagawa R, Melander F, Kastan MB, Bartek J, Lukas J. Spatial organization of the mammalian genome surveillance machinery in response to DNA strand breaks. *J Cell Biol.* 2006 Apr 24;173(2):195-206). Adding photosensitisers complicated the system since, as a result, oxidative damage as well as DNA breaks were induced (in addition to PPs and CPDs). Single and double strand breaks can be induced easily by visible light, without oxidative damage, PPs and CPDs (Solarczyk KJ, Zarębski M, Dobrucki JW Inducing local DNA damage by visible light to study chromatin repair. *DNA Repair (Amst).* 2012 Dec 1;11(12):996-1002), therefore there is no need to use UV and photosensitisers to do achieve this goal. The misleading reasoning which emerges from the Introduction of the submitted manuscript should be corrected for the benefit of those who will use this paper as their first source of information about the techniques of inducing controllable local DNA damage.

As acknowledge in the Reviewer 1's comments, creating mixtures of DNA damage can complicate the interpretation of repair events; however, damage mixtures are created by chemicals as well as micro-irradiation. Photosensitizer are used by a large number of groups to create different damage mixtures for study. Krasin and Hutchinson used bromodeoxyuridine (BrdU) with 313-nm to induce SSBs and lower the yield of DSBs. Rosenstein et al. used BrdU and Hoechst with 365 nm light to introduce SSBs to the DNA. So we were attempting to acknowledge variations on the methods, and their reported applications. We do not use photosensitizers in this work, which we have now better clarified in the introduction.

3. Again, this statement "...numerous reports emerged demonstrating that DNA strand breaks could be induced with and without sensitizers in the UV-A range and even at 405 nm" (line 92-3) by saying "UV-A... and even by 405nm" the authors seem to suggest that even as long a wavelength as 405 can induce DNA breaks. They are ignoring the fact that, as mentioned above, it is well known now that SSBs and DSBs can be induced by visible light of much longer wavelength (for instance 488nm) and low intensity.

We have revised the language of this section.

4. The authors state that "in order to discriminate between SSBs and DSBs, or between DNA repair pathways, users must carefully control the applied power over a specific section of the nucleus..." I fully agree with this statement. However, the authors do not comply with their own advice. Intensities of light and total doses of energy they used are not disclosed anywhere. These values (in mW and uJ) must be measured and disclosed to make this paper useful.

We have now added a section in the protocol 3.7 describing how the applied laser dose can be measured, and the doses used for our damaging conditions.

5. The authors state that they used lens "20× C-Apochromat (NA 1.2) air immersion objective". Such a lens does not exist. If NA is 1.2 and this is a dry lens (air) sinus alpha would have to be 1.2. The authors will agree with the reviewer that sinus

alpha does not exceed a value of 1.

We thank the reviewer for point out this mistake, which we have now corrected.

6. One of the most important points of this paper, a detailed description of the method of applying light to the selected area of nucleus, is missing (very surprising for a methodology paper). Lines 139-140 are all there is. This should be corrected. The reader must be given the scanned area (in a confocal plane), the speed of scanning, the mode of scanning (raster, interlaced, etc.), the total time of exposure, and most importantly - the intensity of light beam emerging out of the objective lens, and the resulting total dose of light delivered to the selected area of the sample (nucleus). Providing the pinhole size makes no sense (line 141). Confocal pinhole is located in front of the detector and has no influence on the intensity and dose of light that induce DNA damage.

We have added in the necessary details as suggested by the reviewer. The pinhole was included as a general image condition, which is why it was separate from the micro-irradiation. The cells must be located and imaged prior to damage induction.

7. Another shortcoming of the manner in which the authors explain their approach is the way they describe their fluorescence detection conditions. They talk about "the fluorescence channel for the protein of interest (i.e., 488 nm for GFP, 561 nm for RFP)" (line 182). These are not fluorescence channels. 488nm is the (argon) line excitation wavelength for GFP, 561nm is the line they must have used to excite RFP. The excitation and emission conditions should be described properly.

We have specified the imaging conditions for clearly in the protocol.

8. The authors state "355 nm stimulation occurred at 100% laser power over 2 and 10 seconds, and 405 nm laser excitation occurred at 100% laser power at 8 and 0.5 frames per second (fps)." (lines 189-191, also lines 309-310). Also, in lines 433 and 434 they talk about dose of light measured in seconds and frequency of pulses. The same in Fig. 2. The only acceptable way of describing these experimental conditions is to provide the light intensity in Watts/m², and the total dose in Joules. This is the only way others can try to reproduce this methodology. Note that 100% laser means nothing, even for the same type of instrument. The terms 'stimulation' and 'excitation' are also wrong in this context.

We have included the information requested by the reviewer.

9. The authors talk about γ H2AX as a marker of DSBs. Again, the current knowledge includes information indicating that this is not the case (Cleaver JE, Feeney L, Revet I. Phosphorylated H2Ax is not an unambiguous marker for DNA double strand breaks. Cell Cycle. 2011; 10:3223-4; Rybak P, Hoang A, Bujnowicz L, Bernas T, Berniak K, Zarębski M, Darzynkiewicz Z, Dobrucki J. Low level phosphorylation of histone H2AX on serine 139 (γ H2AX) is not associated with DNA double-strand

breaks. Oncotarget. 2016 Aug 2;7(31):49574-49587). These facts should be taken into account and mentioned in the text. Moreover, the authors ignore the fact that recruitment of repair factors is not always a proof of DNA damage (Pankotai T, Hoffbeck AS, Boumendil C, Soutoglou E. DNA damage response in the absence of DNA lesions continued. Cell Cycle. 2009; 8:4112-4018. This limitation should be mentioned in the paper.

We agree with the reviewer that gH2AX is a strand break marker rather than a DSB marker, but surely the reviewer would agree the bulk of the literature using gH2AX as a specific marker for DSB. To address this issue, we have pointed out the issues with using gH2AX as a strand break marker, including the issue of pan nuclear staining, which was mentioned by Reviewer 1. Additionally, we have used 53BP-1 as an additional DSB marker to help clarify the point and suggest the users incorporate more than one marker for their characterization studies, when possible.

10. Images in Fig. 1 should be accompanied by fluorescence intensity profiles so that the real levels of accumulation and signal noise can be seen.

We have revised the figure to provide a scatter plot to better illustrate the fluorescence signal above background.

11. The traces in Fig. 3 should start at a time before damage induction, as the authors advise their readers to do.

We have revised the figure to better indicate to the reader that the 0 time is pre-irradiation.

12. In the legend to Fig. 3 the authors should explain what they mean by saying fluorescence intensity - is it average? integrated? maximum?

As suggested by all of the reviewers, we have clarified the analysis procedure and included a figure to clarify how the fluorescence intensity is measured and reported.

Reviewer #3:

Major Concerns:

While it is claimed that different lasers (355 nm and 405 nm) can be used to generate a specific kind of DNA damage, the results presented are not really convincing. While the involvement of XRCC1 in the repair of both single and double strand breaks is discussed in the introduction, when presenting the results it is considered that the recruitment of XRCC1-GFP corresponds to single strand breaks only, I'm just wondering how can we be so sure? Furthermore, concerning the induction of double strand breaks, while it is discussed in the introduction the requirement of adding sensitizers for the generation of this kind of damage, the formation of γ H2AX is observed in all the conditions used without the addition of

any DNA intercalator. The sentence: "Here, laser micro-irradiation is performed to examine repair of SSBs and DSBs induced by two common confocal laser wavelengths, 355 nm and 405 nm, and characterization of the applied laser power is described for inducing specific damage mixtures" does not really correspond to the results presented and should be changed. So in this case it should be concluded that a mixture of different kind of damages are induced with both lasers. A major consideration concerns the use of CHO and MEF cells that is not clear for me: Is there any specific reason to use CHO-K1? why not to use the WT CHO cells or the CHO cells lacking XRCC1 (such as EM9 or EM-C11)? If you really want to compare the results in the presence or absence of the endogenous XRCC1 protein, should be more useful to use the same cell type rather than comparing CHO with MEF. Concerning the sentence: "The resolution of the 10s 355 nm dose by the *Xrcc1*^{-/-} MEFs may be a function of the lack of endogenous competing *Xrcc1*" (Lines 443-444), I do not really understand your argument: the release of XRCC1-GFP is even faster in MEF cells that do not have the endogenous protein. You argue for a difference of those cells while they behave exactly the same than CHO cells with the 405 nm laser, how do you explain that? As mentioned before, I think that to compare the results in the presence or absence of the endogenous XRCC1 protein, you should use the same cell line with or without the protein rather than comparing CHO with MEF cells. Anyway, the idea here is to describe a detailed protocol, not to discuss scientific results; this part is really confusing so I would suggest removing this comparison between CHO and MEF and just showing one graph as an example to illustrate how to measure the kinetics of DNA repair proteins recruitment and release. In general I think that the protocol is extremely long and several things are repeated more than once. I would suggest you to simplify for more clarity.

Many of the issues brought up here echo the other reviewers, so we refer to our responses in those sections. We have significantly revised and clarified the manuscript to address the issues of mixtures, issues of specificity in repair pathways, and markers chosen. We have also removed the MEF cell lines from the manuscript as the reviewer suggested to simplify the results. We hope these additions to the text and simplification better highlight the method and the results it generated. As to the length of the protocol, in order to make the method generalizable and useful to the journal's audience we had to be very specific about the methods utilized, and given the large number of comments and additions requested by the reviewers, we feel the final protocol will allow inexperienced users to learn the technique and avoid issues in their experimental design that would preclude publications later on.

Some remarks concerning the figures:

Figure 1. Images of the cells before micro-irradiation should be included. As a suggestion for the part B, it would be better to use dual-color microscopy to do the IF with the corresponding antibodies (using a secondary antibody coupled to Alexa 546 for example) in cells expressing XRCC1-GFP to perfectly localize the site of the damage.

We have included the pre-micro-irradiation images in the figure.

Figure 2. Images should be included to illustrate the quantification results presented. Several observations presented in

this figure require further discussion: How do you explain the increase in γ H2AX signal observed 40 min after micro-irradiation for the conditions 355nm (2 sec) and 405 nm (0.5 fps). Another surprising thing is the higher level of signal observed when 405 nm laser is used at 0.5 fps, it was the opposite in the case of XRCC1-GFP. Do you have any explanation for those observations? It would be useful to discuss about that.

We have revised Figure 1 to include the quantification procedure as suggested.

Other additional aspects that are not covered by the protocol and that look important to me are:

- Should be included how to monitor for bleaching of the fluorescence signals

We have now addressed this in Line 246-252.

- Nothing is mentioned concerning transfection of the cells (amount of plasmid used, protocol used for transfection, even if they are stable transfected cells could be useful to include this information).

We have now added to section 1 so the cell line generation is included.

Minor Concerns:

The introduction is quite complete and well-illustrated; just some other references should be added mostly concerning the induction of base-modifications. Line 75: The reference 7 (Limoli and Ward, 1993) describes the induction of DSB by the addition of BrdU and it is not the most appropriate for the discussion of the induction of base modifications. Authors should include other references to illustrate this aspect: such as Menoni et al., J Cell Biol. 2012 and Campalans et al., Nucleic Acids Res. 2013.

We have corrected this oversight and included the suggested references.

Several mistakes have been found in the protocol and should be corrected carefully. I will try to point here several aspects that from my point of view are missing or unclear:

Line 130. Is there a particular reason to use different objectives for the different lasers? The 40x is not compatible with both systems?

As noted in the comments for reviewer 1, we have made this correction.

Line 134. You should say dry objectives and not air immersion objective.

We have made this correction.

Line 140-141. The sentence: "In the presented system, cells are micro-irradiated and imaged using a scan resolution of 1024x1024 pixels with 1x confocal zoom, with the pinhole set to 69 μ m" should be moved to the part 3.5 concerning micro-irradiation (line 187).



This information was included in the earlier section (2.3) because the protocol uses these settings to image the sample for focus and the intervening steps, so we believe the information is in the appropriate place.

Line 141. Please mention also the AU (airy units) corresponding to this pinhole size.

We have made this correction.

Line 151. The part 3.2 concerning registration of image fields is extremely long and should be simplified.

Registration is a significant issue in the micro-irradiation field, and it is never adequately addressed in publications. We believe it is essential to include this detailed information, and it was noted by reviewer 1 as “valuable”.

Line 182 and 183. Specify that the mentioned nm (488 and 561) correspond to the wavelength of the lasers used for excitation of the fluorochromes.

We have made this correction.

Line 187. Include the size of the ROI used for microirradiation.

This information was already specified in the protocol in line 209.

Line 190. Mention the % of laser is not a very useful information because this will depend on each system. You should mention the real laser power measured at the objective.

We have included this information in section 3.7.

Line 212. Use Immunofluorescence and not IF in the title.

We have made this correction.

Line 248. Fix and permeabilize cells in ice cold methanol.

We have made this correction.

Line 268. Replace 8-oxdG by 8-oxodG or 8-OHdG

We have made this correction.

Line 275. Mention concentration of the stock for DAPI (10 mg/ml as mentioned in line 233)

We have made this correction.

Line 289. Replace "correspond" by "corresponds"



We have made this correction.

Line 292. Make reference to part 3.2

We have made this correction.

Line 308. You should avoid speaking about fluorescent channels when mentioning the wavelength of the lasers used for the excitation. Please be careful with this mistake that is all over the protocol.

We have clarified the imaging conditions and the laser wavelengths used throughout the protocol.

Line 336. Please specify the appropriate ImageJ plugins that are suitable for tracking. Tracking is mentioned but no explanation on how to do it is included, I think it would be of interest to include this information.

There are a large number of protocols and it would be more appropriate for users to find one they are comfortable with, so we included the resources library for their reference

Line 350. Replace for "Analyze protein recruitment in fixed cells by immunofluorescence"

This clearly delineates the two sections, so we have kept this line.

Line 388. Please correct "generated" to "generate".

We have made this correction.

Line 388. "Focus with XRCC1-GFP" should be replaced by "focus of XRCC1-GFP".

We have made this correction.

Line 392. Missing information: 8 fps you should specify the number of frames or the time (otherwise this point is not clear).

We have clarified this point.

Line 405. Please be careful when speaking about "micro-irradiation powers" because if I understood it correctly the power

is always set at 100%, what is changing is the time of exposure/dose isn't it?

We have revised the language to refer to combinations of power and time as dose throughout the manuscript to clarify this issue.

Line 406. Please avoid speaking about recruitment when mentioning γ H2AX, it is not a recruitment but a phosphorylation of a protein that is already present. Replace by formation of γ H2AX or phosphorylation of H2AX.

We have made this correction.

Line 424. Replace "recruit" by "are recruited"

We have made this correction.

Line 484. Replace "used for characterizing damage response" by "used for characterizing cellular responses to the induction of DNA damage"

We have made this correction.

Line 516. Replace « post-translation » by « post-translational »

We have made this correction.

Line 531. Replace « utilized » by « used »

We have made this correction.

List of Material/Equipment- We have made the corrections suggested to the table listed here.

The list needs to be reorganized in order to group the different elements in a logical way: for example both cell lines (CHO-K1 and MEF) should be mentioned together and the same is true for the laser sources (it is weird to have one in the first position and the other one in position 15 in the list). As a suggestion for more clarity I propose the following order:

Microscope, lasers and softwares:

Nikon A1rsi laser scanning confocal microscope Nikon
355 nm laser PicoQuant VisUV S175C Radiation source
Galvonometer photoactivation miniscanner Bruker
Microscope slide power meter THORLabs
NIS Elements software Nikon

Cell lines and culture:

1660 Springhill Avenue
Mobile, AL 36604-1405

Comprehensive Oncology Healthcare & Research

Tel: (251) 460-6993
Fax: (251) 460-6994



CHO-K1 From Dr. Samuel H. Wilson, NIEHS
XRCC1-/- p53-/- MEFs From Dr. Robert Tebbs, LLNL
4 chambered coverglass ThermoFisher 155382
8 chambered coverglass ThermoFisher 155409

Plasmids:

XRCC1-GFP Origene RG204952

Xrcc1-GFP From Dr. Samuel H. Wilson, NIEHS

(mention origin, human/mouse. Provide accession numbers and details of the plasmids)

Transfection?? Nothing is mentioned concerning this point and should be added!!

Antibodies:

Anti 8-oxo-2'-deoxyguanosine Trevigen 4354-MC-050

Anti cyclobutane pyrimidine dimer Cosmo Bio clone CAC-NM-DND-001

Anti-phospho-histone H2AX Millipore 05-636-I

Alexa 488 goat anti-mouse ThermoFisher A11029

Alexa 546 goat anti-rabbit ThermoFisher A11010 (not used in the protocol!!)

Reagents:

37% Formaldehyde ThermoFisher 9311 Caution toxic!

Methanol VWR BDH1135 Caution toxic!

HCl Fisher SA49

Bovine serum albumin (BSA) Jackson Immuno Research 001-000-162

Normal goat serum ThermoFisher 31873

Phosphate buffered saline ThermoFisher 0780

Sodium azide Sigma-Aldrich S2002 Caution toxic!

Tris Hydrochloride Amresco O234

Triton X-100 Sigma-Aldrich T8787

As a general comment several products are indicated with CAUTION in brackets, always referring to the same sentence:

"Wear proper personal protective equipment and dispose the corrosive substance as instructed by institutional environmental health and safety procedures" that is mentioned several times along the protocol. This should be mentioned only once, for example at the end of the list concerning Material/ Equipment.

Some controversies are found, several materials listed in this part are not described in the protocol:

- Alexa 546 goat anti-rabbit is listed but it is not used in the protocol.

- Fetal bovine serum

1660 Springhill Avenue
Mobile, AL 36604-1405

Comprehensive Oncology Healthcare & Research

Tel: (251) 460-6993
Fax: (251) 460-6994



- Microscope slide power meter is mentioned in the list but not used in the protocol and I think it is very important to include this step to give an idea about the real laser power used in the micro-irradiation experiments (and not expressed as a %). It would also be useful to mention the theoretical laser power at the exit of the fiber.

Again, we thank the reviewers for their thorough comments.

Sincerely,

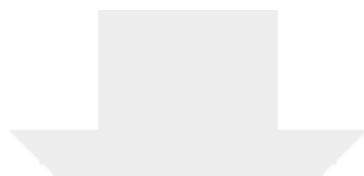
Natalie R. Gassman

Assistant Professor of Oncological Sciences

1660 Springhill Avenue
Mobile, AL 36604-1405

Comprehensive Oncology Healthcare & Research

Tel: (251) 460-6993
Fax: (251) 460-6994



[Click here to access/download](#)

Supplemental File

JoVe_Revisions_051217_Final_v2.doc

